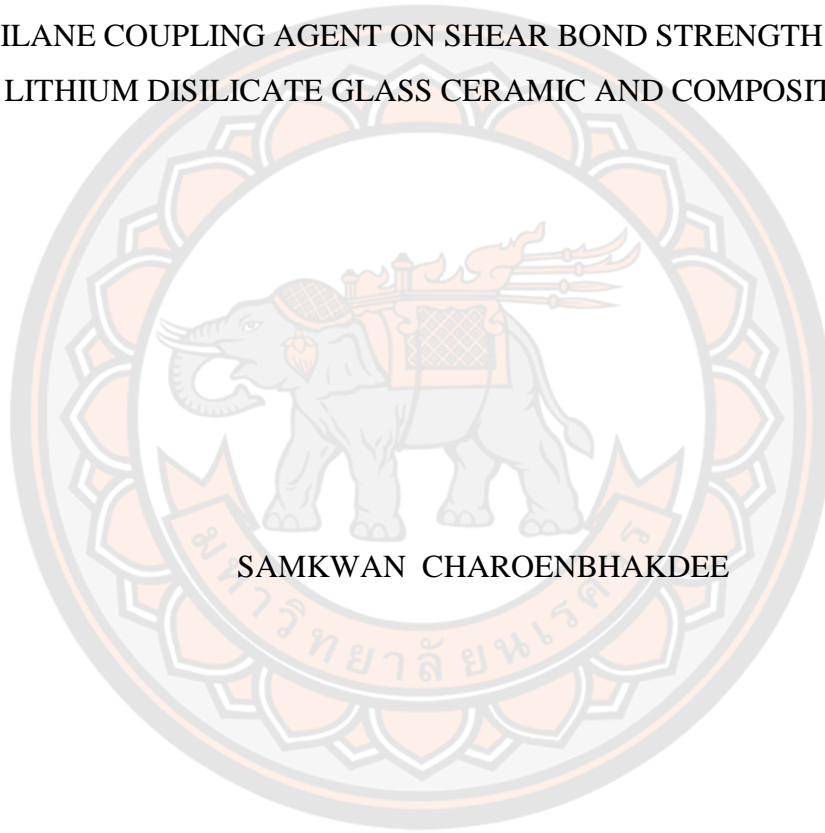




THE EFFECT OF VARIOUS CONCENTRATIONS AND SHELF LIFE OF  
SILANE COUPLING AGENT ON SHEAR BOND STRENGTH BETWEEN  
LITHIUM DISILICATE GLASS CERAMIC AND COMPOSITE RESIN.



SAMKWAN CHAROENBHAKDEE

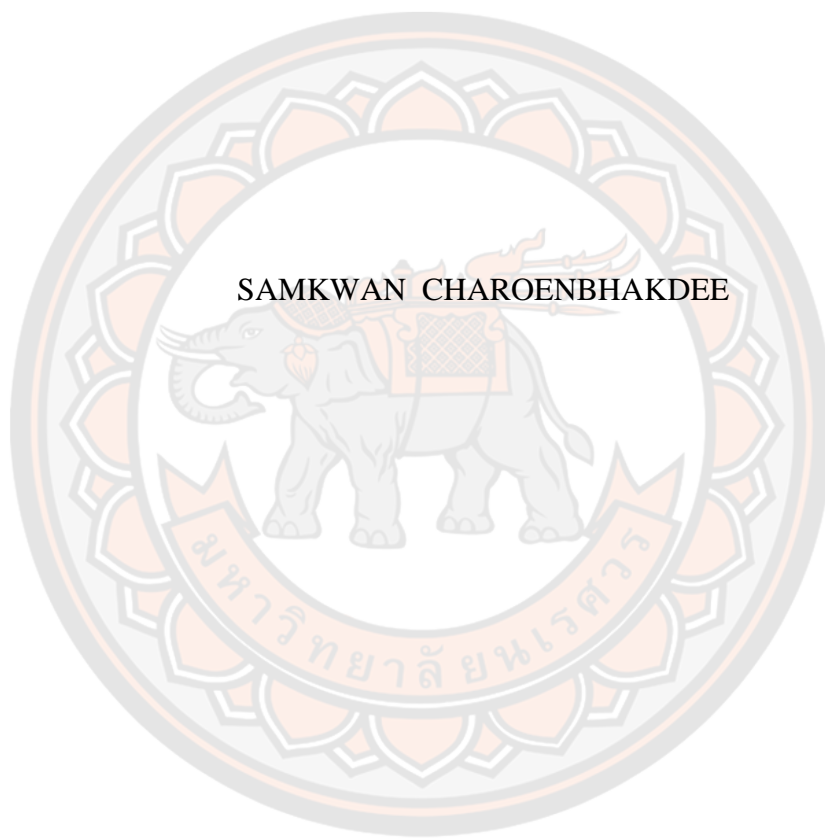
A Thesis Submitted to the Graduate School of Naresuan University  
in Partial Fulfillment of the Requirements  
for the Master of Science in (Master of Sciences in Dentistry (Prosthodontics) - Type

A 2)

2021

Copyright by Naresuan University

THE EFFECT OF VARIOUS CONCENTRATIONS AND SHELF LIFE OF  
SILANE COUPLING AGENT ON SHEAR BOND STRENGTH BETWEEN  
LITHIUM DISILICATE GLASS CERAMIC AND COMPOSITE RESIN.



SAMKWAN CHAROENBHAKDEE

A Thesis Submitted to the Graduate School of Naresuan University  
in Partial Fulfillment of the Requirements  
for the Master of Science in (Master of Sciences in Dentistry (Prosthodontics) - Type  
A 2)  
2021  
Copyright by Naresuan University

Thesis entitled "The effect of various concentrations and shelf life of silane coupling agent on shear bond strength between lithium disilicate glass ceramic and composite resin."

By SAMKWAN CHAROENBHAKDEE

has been approved by the Graduate School as partial fulfillment of the requirements for the Master of Science in Master of Sciences in Dentistry (Prosthodontics) - Type A 2 of Naresuan University

**Oral Defense Committee**

..... Chair  
(Assistant Professor Pisaisit Chaijareenont, Ph.D.)

..... Advisor  
( Pornpot Jiangkongkho, Ph.D.)

..... Internal Examiner  
(Assistant Professor Jadesada Palasuk, Ph.D.)

..... Internal Examiner  
( Yosnarong Sirimethawong, Ph.D.)

**Approved**

.....  
(Professor Paisarn Muneesawang, Ph.D.)

Dean of the Graduate School

**Title** THE EFFECT OF VARIOUS CONCENTRATIONS AND SHELF LIFE OF SILANE COUPLING AGENT ON SHEAR BOND STRENGTH BETWEEN LITHIUM DISILICATE GLASS CERAMIC AND COMPOSITE RESIN.

**Author** SAMKWAN CHAROENBHAKDEE

**Advisor** Pornpot Jiangkongkho, Ph.D.

**Academic Paper** M.S. Thesis in Master of Sciences in Dentistry (Prosthodontics) - Type A 2, Naresuan University, 2021

**Keywords** Silane coupling agent, Shear bond strength, Lithium disilicate glass ceramic, Composite resin, Silanization

### ABSTRACT

**Objective:** To evaluate the shear bond strength of various concentrations of silane coupling agents between lithium disilicate glass (LDS) ceramic and composite resin.

**Materials and Methods:** Seven groups (n=7) of experimental silane coupling (ESC) agent, including 1%, 3%, 6%, 9%, and 12% (v/v) concentrations, were prepared for silanization and non-silanization (NS) and commercial silane coupling (CSC) agent groups served as controls. The shelf life of ESCs was evaluated at 0, 1, 2, 4, 8, 16, and 32 days after hydrolysis. Shear bond strength test was performed. The mode of failure, fracture surface topography, and elemental analysis were evaluated.

**Results:** The mean shear bond strength of NS, CSC, and ESC groups in non-thermocycling and thermocycling ranged from 7.3 to 26.3 and 1.8 to 18.2 MPa, respectively. The results were statistically analyzed using Two-way ANOVA, followed by Tukey's multiple comparison test ( $\alpha=0.05$ ). These results showed that the shear bond strength of the NS group (1.8 MPa) after thermocycling was significantly lower than that of the ESC and CSC groups, while the 6% ESC group (18.2 MPa) showed a higher shear bond strength than the other groups. The mean shear bond strengths after 0, 1, 2, 4, 8, 16, and 32 days of hydrolyzing 6% ESC ranged from 13.7

to 18.2 MPa.

Conclusions: The 6% ESC group had the highest shear bond strength. The shear bond strength decreased significantly after the thermocycling. The shear bond strength of the hydrolyzed silane coupling agent gradually decreased after being hydrolyzed over time after hydrolysis.



## ACKNOWLEDGEMENTS

I would like to acknowledge my advisor, Dr. Pornpot Jiangkongkho for his invaluable advice and encouragement throughout this thesis. I am grateful to Ass. Prof. Dr. Jadesada Palasuk and Dr. Yosnarong Sirimethawong, the internal examiner of my thesis defense for their advice. I express a special thank to Asst. Prof. Dr. Pisaisit Chaijareenont, the external examiner of my thesis defense.

I wish to express my special thank to Thawangpha hospital for giving me the chance to study in the Master Degree Program.

I would like to thank PC Dental Lab for donating the lithium disilicate glass - ceramic materials to this experiment.

I am grateful to the Hard tissue specimen preparation laboratory, the Biomaterial testing laboratory and the Dental laboratory under the Laboratory Unit Faculty of Dentistry of Naresuan University for their helpful in all procedures in this thesis.

Finally, I am greatly thankful to my parents, my sister, and my brother for their love, encouragement and all support throughout my life.

SAMKWAN CHAROENBHAKDEE

## TABLE OF CONTENTS

	<b>Page</b>
ABSTRACT.....	C
ACKNOWLEDGEMENTS.....	E
TABLE OF CONTENTS.....	F
LIST OF TABLES.....	H
LIST OF FIGURES.....	I
CHAPTER I INTRODUCTION.....	1
CHAPTER II OBJECTIVES.....	4
CHAPTER III LITERATURE REVIEW.....	5
1 Dental Ceramics.....	5
2 Silane coupling agent.....	7
3 Shear bond strength.....	11
4 Thermocycling.....	11
5 Scanning electron microscopy.....	12
CHAPTER IV MATERIALS AND METHODS.....	13
Part I: The various concentrations of ESC and thermocycling challenge.....	15
1.1 The specimens preparation.....	15
1.2 Silanization process.....	25
1.3 Surface treatment.....	28
1.3.1 HF.....	28
1.3.2 ESC.....	29
1.3.3 Commercial silane coupling agent.....	31
1.4 Adhesive agent.....	31
1.5 Composite resin.....	33
1.6 Non-thermocycling and thermocycling challenge.....	34
1.7 Shear bond strength test.....	36

1.8 Mode of failure analysis .....	38
1.9 Scanning electron microscopy (SEM).....	40
Part II: The shelf life of hydrolyzed silane coupling agent. ....	40
1 Shelf life of hydrolyzed silane coupling agent.....	40
Part III: The Elemental analysis. ....	40
1 Elemental analysis .....	40
Statistical analysis.....	43
CHAPTER V RESULTS .....	44
1 The surface roughness (Ra) of lithium disilicate glass ceramic .....	44
2 The various concentration of ESC and thermocycling challenge.....	44
3 Mode of failure analysis .....	46
4 The shelf life of hydrolyzed silane coupling agent.....	47
5 The elemental analysis.....	48
CHAPTER VI CONCLUSIONS .....	57
REFERENCES .....	58
BIOGRAPHY .....	64

## LIST OF TABLES

	<b>Page</b>
Table 1 The commercial silane coupling agents.....	9
Table 2 The silane coupling agent, solutions, ceramic, and materials used in the present study and their manufacture .....	13
Table 3 The experimental groups in this study .....	25
Table 4 The amount of ETH and MPS in each ESC group .....	25
Table 5 The means and standard deviations of the Ra value .....	44
Table 6 The means and standard deviations of shear bond strength in non-thermocycling and thermocycling conditions .....	45
Table 7 Mode of failures and means percentage of composite resin remnants of experimental LDS specimens in non-thermocycling and thermocycling conditions (n=7).....	47
Table 8 The means and standard deviations of the shear bond strength of hydrolyzed 6% ESC.....	48

## LIST OF FIGURES

	<b>Page</b>
Figure 1 The tetrahedral configuration of ceramic. ....	6
Figure 2 The LDS specimens (A: the lateral view, B: the top view).....	15
Figure 3 .The LDS specimens were cut into 13.0 mm in diameter and 2.0 mm in thickness (A: the top view, B: the lateral view).....	16
Figure 4 The low-speed diamond saw. ....	17
Figure 5 The stereomicroscope.....	18
Figure 6 A: The LDS specimens surface under 6 magnification using stereomicroscope, B: The crack surface on the LDS specimens. ....	19
Figure 7 The 2 millimeter-thickness of LDS specimens were placed into the polyvinylchloride cylindrical mold (20.0x15.0 mm) with auto-polymerized acrylic resin (A: the top view, B: the lateral view).....	21
Figure 8 The polishing machine. ....	22
Figure 9 An ultrasonic cleaner device. ....	22
Figure 10 An atomic force microscopy. ....	23
Figure 11 A double-sided adhesive tape with a 5 millimeter-diameter hole was placed on the LDS specimens. ....	24
Figure 12 The 99.9% (v/v) ETH.....	26
Figure 13 The 98% (v/v) of MPS.....	26
Figure 14 A: The magnetic stirrer, B: The hydrolysis process of ESC was performed using the magnetic stirrer.....	27
Figure 15 A: The 9% hydrofluoric acid, B: The surface treatment of LDS specimens with 9% hydrofluoric acid. ....	28
Figure 16 The bonding area of LDS specimens after surface treatment with 9% hydrofluoric acid.....	29

Figure 17 A: The micropipette, B: The application of the 50 microliters of CSC and each concentration of ESC on the bonding area of LDS specimens use by micropipette. ....	30
Figure 18 The commercial silane coupling agent. ....	31
Figure 19 The adhesive agent. ....	32
Figure 20 The LED light-curing unit. ....	32
Figure 21 The 3.0 millimeter-height of polyvinylchloride tube was placed over the bonding area and act as the composite resin mold. ....	33
Figure 22 The flowable composite resin. ....	34
Figure 23 The dry electronic cabinet. ....	35
Figure 24 The thermocycling apparatus. ....	35
Figure 25 The universal testing machines. ....	37
Figure 26 Set-up the LDS specimens for shear bond test. ....	38
Figure 27 The fracture surface of LDS specimens after shear bond strength test under the stereomicroscope, A: The adhesive failure, B: the mixed failure mode, Red dash circle represent bonding area, White arrow represent composite resin remnants. ....	39
Figure 28 The tetrahydrofuran. ....	41
Figure 29 The spectrophotometer. ....	41
Figure 30 Experimental procedure schematic. ....	42
Figure 31 The atomic percentages of C atom on the surface of LDS specimens in unwashed THF and washed THF conditions. ....	49
Figure 32 Representative SEM images of the fractured LDS surfaces in non-thermocycling condition. A1, A2: Non-etched LDS surface, B1: The etched LDS surface. White arrow showed the etched pattern, B2: The etched LDS surface. White arrow showed the lithium disilicate glass particles, C1, C2: Non-silanized LDS surface, D1, D2: The fractured surface of the CSC group, E1, E2: The fractured surface of 1% ESC, F1, F2: The fractured surface of 3% ESC, G1, G2: The fractured surface of 6% ESC, H1, H2: The fractured surface of 9% ESC, I1, I2: The fractured surface of 12% ESC. F1-H2: Black arrows showed the remaining composite resin, 1:500 magnification, 2: 5,000 magnification. ....	53
Figure 33 Representative 5000 magnifications of SEM images on the LDS surfaces. A: etched LDS surfaces, B: etched and silanized with 6% ESC, A and B showed exposed needle-like crystal of LDS, C: etched and silanized with 12% ESC. White	

circle showed the cluster-crystal structure of LDS that was covered with physisorbed layers.....54

Figure 34 Representative SEM images of the fractured LDS surfaces in thermocycling condition. A1, A2: Non-silanized LDS surface, B1, B2: The fractured surface of the CSC group, C1, C2: The fractured surface of 1% ESC, D1, D2: The fractured surface of 3% ESC, E1, E2: The fractured surface of 6% ESC, F1, F2: The fractured surface of 9% ESC, G1, G2: The fractured surface of 12% ESC. D1-F2: Black arrows showed the remaining composite resin, 1: 500 magnification, 2: 5,000 magnification .....55



# CHAPTER I

## INTRODUCTION

Ceramic restorations were introduced in the 1980s [1] and thereafter, they have been widely used in dentistry owing to their natural appearance, chemical stability, biocompatibility [2], high compressive strength, and a coefficient of thermal expansion similar to that of the tooth structure [3]. The esthetic appearance of all ceramic restorations is superior than that of porcelain-fused-to-metal restorations [4]. The mechanical properties of lithium disilicate glass ceramic (LDS), which is a second-generation silica-based ceramic, are better than those of the first-generation silica-based ceramics. Furthermore, LDS is highly translucent and can mimic natural tooth colors. Therefore, they are considered as the most promising alternatives for restoring tooth structure [3].

The clinical success rate of all ceramic restorations depends on the quality of cementation [5]. In cementation, the bond between the ceramic restoration and tooth structure consists of two parts: the tooth surface-adhesive agent and the adhesive agent-ceramic surface. The shear bond strength between the adhesive agent and the ceramic surface plays a crucial role in clinical success [3].

Ceramic surface treatments can be divided into mechanical and chemical surface treatments [6]. Mechanical surface treatments, such as sandblasting and chemical etching, can create micromechanical retention on the ceramic surface, which leads to bonding with the adhesive agents [7, 8]. However, sandblast surface treatment is not recommended due to the insufficient bond strength with silica-based ceramics [3, 5]. Chemical surface treatment involves etching with hydrofluoric acid (HF) at various concentrations between 8 and 10% for 2 to 2.5 min depending on the manufacturer's instructions. The micro-morphologic change after HF etching can create a honeycomb-like topography on the ceramic surface, resulting in micromechanical retention [3, 8]. Chemical surface treatment also involves the application of a silane coupling agent, which is a major bonding agent, that provides a chemical bond to silica-based ceramics [7]. Therefore, the recommended surface

treatment to achieve high bond strength is HF etching, which performs micromechanical retention, as well as silane coupling agent that produces the chemical bond [3, 9].

Silane coupling agent is a bifunctional molecule that acts as an adhesive agent between the inorganic particles, i.e., silicon oxide on the ceramic surface, and the organic substance of the adhesive agent matrix. The silane coupling agent widely used in dentistry is  $\gamma$ -methacryloyloxypropyltrimethoxysilane (MPS) [10]. It has short chain and low molecular weight molecules that can minimize the homocondensation of MPS [7]. In addition, it has a minimal color effect from its refractive index (1.43) [11], which is similar to that of the ceramic materials (1.45) [12]. In previous studies, different concentrations of silane coupling agents have been varied between 1 and 10% (v/v) [10, 13]. The 5% (v/v) MPS provided the highest shear bond strength after treatment with glass or resin materials [14], whereas that between polymethylmethacrylate (PMMA) and alumina plate that were silanized with 1% (v/v) MPS in 70% (v/v) ethanol resulted in a statistically significant shear bond strength [15]. However, the appropriate concentration of the silane coupling agent on the shear bond strength between the ceramic and composite resin remains controversial.

The effects of the silane coupling agent depend on the silane concentration, solution, temperature, and shelf life [16]. The shelf life of the hydrolyzed silane coupling agent is an important factor affecting the shear bond strength. After the silane coupling agent was hydrolyzed, it changed to an active form (hydrolyzed silane coupling agent) and tended to undergo homocondensation. In homocondensation, the silane coupling agent can react with the silica surface; however, the quality of the bond strength is unpredictable [17]. Previous studies on the shelf life of silane coupling agents after hydrolysis were inconclusive.

Therefore, this study aims to investigate the shear bond strength of various concentrations of experimental silane coupling agent (ESC) between LDS and composite resin under non-thermocycling and thermocycling conditions, as well as the effect of the shelf life of the hydrolyzed silane coupling agent on the shear bond strength between LDS and composite resin. The null hypotheses were that there would be no significant differences in the shear bond strength between LDS and composite resin with various concentrations of silane coupling agent and thermocycling challenge. There would be no significant differences in the shear bond strength

between LDS and composite resin after 0, 1, 2, 4, 8, 16, and 32 days of hydrolysis of the silane coupling agent.



## **CHAPTER II**

### **OBJECTIVES**

In order to contribute a better understanding about the application of silane coupling agents on shear bond strength between silica-based ceramic and resin matrix materials, we examined the appropriate concentration of silane coupling agent and the shelf life of hydrolyzed silane coupling agent, affect the shear bond strength of lithium disilicate glass-ceramic and composite resin materials. The specific objectives of these studies were as follows:

1. To investigate the effect of different concentrations of silane coupling agent on shear bond strength between lithium disilicate glass ceramics and composite resin.
2. To investigate the effect of shelf life of hydrolyzed silane coupling agent and shear bond strength between lithium disilicate glass ceramics and composite resin.

## **CHAPTER III**

### **LITERATURE REVIEW**

#### **1 Dental Ceramics**

Ceramics is one of the four major classes in dental materials used to replace porcelain fused to metal restorations. The improvement of mechanical properties and manufacturing methods can be used in the restoration of damaged tooth structures or replace missing teeth in both anterior and posterior regions [18]. The basic structure of dental ceramics based on silica structure contains glassy phases and crystalline phases. The glassy phases improve the translucency but allow crack propagation to occur. On the other hand, the dispersion hardening of crystalline phases results in mechanical properties improvement and decreases crack propagation [2, 18]. Therefore, the mechanical and optical properties of dental ceramics mainly depend on the presence of the amount of crystalline phase [18].

Considering the chemical structure of dental ceramic, a single unit of silica bond with 4 oxygen atoms both covalent and ionic bond, forming tetrahedral configuration thus making it stable (Figure 1), excellent thermal characteristics, optical insulating characteristics, good resistance to the compressive strength, and inertness translucency. However, this strong dual bond may also impart brittle due to the glass matrix leading to the fracture even at low tensile stress applications [18].

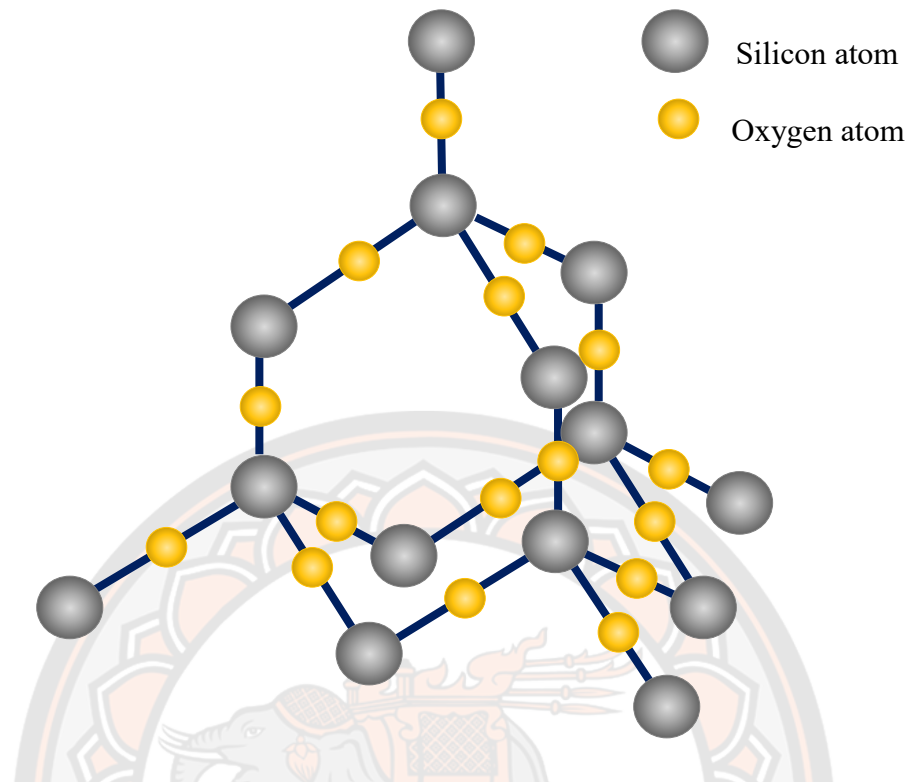


**Figure 1 The tetrahedral configuration of ceramic.**

The classification of dental all ceramic materials

1. Classification based on processing technique
  - 1.1 Powder/liquid, glass-based systems
  - 1.2 Machinable or pressable blocks of glass-based systems.
  - 1.3 CAD/CAM or slurry, die-processed, mostly crystalline (alumina or zirconia) systems
2. Classification by fracture toughness
3. Classification by microstructure (i.e. amount and type of crystalline phase and glass composition). The microstructure level of ceramics can be defined by glass-to-crystalline ratio into 4 basic compositional categories
  - 3.1 Glass-based systems (mainly silica)
  - 3.2 Glass-based systems (mainly silica) with fillers, usually crystalline (typically leucite or more recently, lithium disilicate)
  - 3.3 Crystalline-based systems with glass fillers (mainly alumina)
  - 3.4 Polycrystalline solids (alumina and zirconia)

Glass-based systems are made from materials that contain mainly silicon dioxide (also known as silica or quartz), various amounts of alumina, that forming aluminosilicates glasses and other minerals such as potassium, sodium, which are known as feldspars. There are many methods to fabricate the dental ceramics in dentistry [19].

The application of resin-bonded ceramic restoration for bridge construction especially in posterior region, a glass ceramic based on a  $\text{SiO}_2\text{-Li}_2\text{O}$  system has been developed which is called the IPS Empress II (Empress II, Ivoclar-Vivadent) through a combination of the lost-wax and heat-pressed technique [5]. The manufacturers have added the crystalline filler particles to increase the strength, thermal expansion and construction behavior of ceramics. It consists of about 70% (v/v) of a lithium disilicate ( $\text{Li}_2\text{Si}_2\text{O}_5$ ) crystal and 30% (v/v) of the glass ceramic. The mechanical properties of LDS are higher than the leucite-glass ceramic, which a flexural strength in the region of 350-450 MPa and fracture toughness approximately three-times higher than the leucite glass ceramic. The glass ceramic is highly translucent due to the optical compatibility between the glassy matrix and the crystalline phase, which minimize internal scattering of the light as it passes through the material [19].

## 2 Silane coupling agent

Silane is a very effective coupling agent to increase the efficiency bond between composite resin and dental restorative materials especially silica-based materials. A general formula for functional silane coupling agent is  $\text{Y-(CH}_2\text{)}_m\text{-Si-(OR)}_3$  [10] which is a bifunctional molecules and can be reacted as a dual reactivity. The organic functional part (e.g. vinyl  $\text{-CH=CH}_2$ ) can be polymerized with an organic matrix. The alkoxy groups (e.g. methoxy  $\text{-O-CH}_3$ , ethoxy  $\text{-O-CH}_2\text{CH}_3$ ) can be reacted with an inorganic substrate to create the covalent bond between the matrix [20].

The functional silane coupling agent can be activated by hydrolysis as shown as the equation before they can bond, via  $\text{-OH}$  groups on the substrate surface.



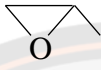
The silane solution is applied on the pretreated substrate surface, the free silanol groups first form hydrogen bonding with the hydroxyl (-OH) groups on the inorganic substrate surface. Then, a -Si-O-(substrate)-linkage is formed between the silanol and “HO-(substrate)” surface by condensation [10]. Silane coupling agents are widely used in various industrial fields. The commercial silane coupling agents product is shown in Table 1 [21, 45, 46]. MPS is the most commonly used in dental laboratory and chairside, usually diluted in water-ethanol solution with acetic acid [20]. They are 2 systems of the application of silane coupling agent which are pre-hydrolyzed and hydrolyzed form. The pre-hydrolyzed form of two-bottle silane solutions is consisting of an unhydrolyzed silane in ethanol in one bottle and the other is an aqueous acetic acid solution. The application of two-bottle systems is mixed the solution to allow hydrolysis of the silane at a low pH before use [10]. Hydrolyzed form in one bottle of silane solution is in a solvent mixture consisting of ethanol and water with the silane content is usually about 1-10 v/v% concentration [13].

The important factor that affects the hydrolysis process is pH value. Previous studies showed that under acidic conditions or alkaline medium conditions, the hydrolysis rate is fast and the rate of condensation is minimizing [10, 13, 22, 23]. However, Nishiyama *et al.* (1987) showed that the hydrolysis and condensation of silane coupling agents are created under neutral conditions [22]. Therefore, the experimental silane coupling agent to the ceramic surface in this study was evaluated under neutral conditions [22-24].

The hydrolysis time varies 5 to 30 min depending on the silane concentration, solution, and temperature [15]. In addition, the hydrolysis rate was not affected by the increase of temperature, but the homocondensation was mainly accelerated. The immediate temperature increases, the silanol groups are drastically decreasing. Therefore, the silane coupling agent should be kept at temperature (RT) (25°C) after the hydrolysis process to minimize homocondensation [25].

However, the hydrolyzed form of silane solutions has a relatively short life due to the homocondensation of silane that appears in cloudy or milky solution after opening and then it cannot be used. However, the pre-hydrolyzed form of silane coupling agent increase their shelf life in comparison to the hydrolyzed form system [10].

**Table 1 The commercial silane coupling agents**

Functional group category	Reactive group	Application
Amino	Cl-	Polyethylene, Polypropylene, Polystyrene, Acrylic, PVC,
	ClOC-	Polycarbonate, Nylon, Urethane, PBT·PET, ABS, Melamine,
		Phenolic, Epoxy, Polyimide, Furan, Sulfur-crosslinked EPDM,
	OCN-	Peroxy-crosslinked EPDM, Nitrile rubber, Neoprene rubber
	HO-	Butyl rubber, Polysulfide, Urethane rubber
	H <sub>2</sub> N-	
	HOSO <sub>2</sub> -	
Epoxy	HOOC-	
	H <sub>2</sub> N-	Polyethylene, Polypropylene, Polystyrene, Acrylic, PVC,
	HO-	Polycarbonate, Nylon, Urethane, PBT·PET, ABS, Melamine, Phenolic, Epoxy, Polyimide,
Mercapto	HOOC-	Diallyl phthalate, Furan, SBR Unsaturated Polyester
	OCN-	Nitrile rubber, Urethane rubber Epichlorohydrin rubber
		Butyl rubber, Polysulfide, Polyethylene, Polypropylene, Polystyrene, PVC, Urethane, ABS, Phenolic, Epoxy, Polybutadiene rubber, Polyisoprene rubber, Sulfur-crosslinked EPDM, Peroxy-crosslinked EPDM,

**Table 1 The commercial silane coupling agents**

Functional group category	Reactive group	Application
Vinyl	$\begin{array}{ccccccc} & & \text{H}_2 & & \text{H}_2 & & \text{H}_2 \\ & &   & &   & &   \\ \diagdown & \text{C} & \diagup & \text{C} & \diagdown & \text{C} & \diagup \\ &   & &   & &   & \\ & \text{H}_2 & & \text{H}_2 & & \text{H}_2 & \end{array}$	Polyethylene, Polypropylene, Diallyl phthalate, Unsaturated Polyester, Sulfur-crosslinked EPDM, Peroxy-crosslinked EPDM
Styryl		Polystyrene, Acrylic
Acryloxy (Meth)	$\begin{array}{c} \text{R}_1 \\   \\ \text{C} = \text{CH}_2 \\   \\ \text{COOR} \end{array}$	Polyethylene, Polypropylene, Polystyrene, Acrylic, Urethane, Polycarbonate, ABS, Diallyl phthalate, Unsaturated Polyester, Sulfur-crosslinked EPDM, Peroxy-crosslinked EPDM
Ureido	$-\text{C}_3\text{H}_6\text{NHCNH}_2$ $\begin{array}{c} \text{O} \\    \\ \text{O} \end{array}$	Nylon, Phenolic, Urethane, Polyimide
Isocyanurate	$\text{H}_2\text{N}-$ <hr/> $\text{HO}-$ <hr/> $\text{HOOC}-$	Polycarbonate, Nylon, Urethane, PBT·PET, ABS, Melamine, Phenolic, Epoxy, Polyimide, Furan, Urethane rubber
Isocyanate	$-\text{C}_3\text{H}_6\text{NCO}$	Polycarbonate, Nylon, Urethane, PBT·PET, ABS, Melamine, Phenolic, Epoxy, Polyimide, Furan, Urethane rubber, SBR, Nitrile rubber, Neoprene rubber, Epichlorohydrin rubber, Polysulfide, Urethane rubber

Additionally, silane coupling agent acts as a wetting agent, which is essential for the intimate contact needed between different materials to increase the resin penetration [26]. Most of silane coupling agent increases the surface energy of ceramic and the wetting ability of resin cements to achieve the highly bonding both physically (by increasing the ceramic surface wetting and making it more receptive to the adhesive) and chemically (by bonding the ceramic to the resin). The water contact angle on the ceramic surface can be reduced, which promotes high surface energy and wettability on surface treatment such as nonthermal plasma [27].

### 3 Shear bond strength

Mastication is a complex sensory-motor activity whereby the ingested food is first transported to the teeth by the tongue and then processed into a bolus for swallowing. Food texture has been shown to affect various aspects of the masticatory process [28]. The biting force can produce the compression force and the tension or shear force that can develop the force along the natural tooth and restorations. The bond strength of the materials at the interface is determined by the shear bond strength [29]. The overloading of shear force resulted in the fracture or dislodge of the restorations, especially veneer or anterior crown. Therefore, the bond strength is extremely important to the success of the restorations [30].

The shear bond strength is calculated following equation [31]:

$$\tau = F/A \text{ (N/mm}^2\text{)},$$

where  $\tau$  is the shear stress ( $\text{N/mm}^2$ ),  $F$  is the applied force ( $N$ ), and  $A$  is the cross-sectional area of the material with area parallel to the applied force vector ( $\text{mm}^2$ ).

### 4 Thermocycling

Thermal cycling is a common procedure that used to investigate the diffusion tracer, shear bond strength and tensile bond strength tests of dental materials. The investigations have used a sensor in specific locations, making comparisons when the samples are in different thermal sites. The majority of reports used hot and cold temperature points which the mean low-temperature point and mean high-temperature point were  $5.0^\circ\text{C}$  and  $55^\circ\text{C}$ , respectively [32]. Dwell times were not clear, but the

mean stated dwell time was 30 seconds [27, 33]. The number of cycles varies from 1 to 1,000,000 cycles which a mean for about 5,000 cycles. In previous studies, no definitive statement of relevant regimen can be made because of wide variation. The frequency of cycles might occur between 20 and 50 times in a day and many reports are mentioned that 5,000 cycles might represent the 6 months in service [33, 34].

## **5 Scanning electron microscopy**

Scanning electron microscopy (SEM) is the most popular technique in the analysis of failed components in the oil and gas industry. The failure modes result from SEM can be easily identified through morphological features obtained from the analysis of the fracture surface [35].

The image formation of a sample is obtained from the secondary electrons (SE) generated through the inelastic interaction that occurs between a primary electron beam and the valence electrons orbiting the nucleus atoms of the sample surface. Then, if SE have sufficient energy, they can depart from the sample surface and be collected by a detector that utilized in image formation [36]. SEM is equipped with an Energy dispersive X-ray spectroscopy (EDS) system to permit the chemical analysis of features observed in the SEM monitor.

The EDS system is mostly used for qualitative analysis of materials in failure analysis cases. Signals production from SEM and EDS system includes the secondary and backscattered electrons that are used in an image forming for morphological analysis [35]. By using a semiconductor detector (SSD: solid-state detector) in the EDS system, it can make an element analysis by immediately converting all of the energy of a characteristics X-ray generated from the specimen into a pulse voltage. EDS can provide not only a qualitative analysis but also a quantitative analysis which has the feature that elemental analysis can be done easily [37].

## CHAPTER IV

### MATERIALS AND METHODS

The silane coupling agent, solutions, ceramic, and materials used and their manufacturers are listed in Table 2. The chemicals were used as received.

**Table 2 The silane coupling agent, solutions, ceramic, and materials used in the present study and their manufacture**

Materials	Concentrations	Code	Brand	Mfg.	Batch No.
<i>Silane coupling agent</i>					
$\gamma$ -methacryloxy propyltri methoxysilane	98.0	MPS	Sigma-Aldrich®	Sigma-Pte Ltd, Mo, USA	SHBK 9588
<i>Solutions</i>					
Ethanol	99.9	ETH	RCI Labscan	RCI Labscan Ltd, Bangkok, Thailand	19110052
Tetrahydrofuran	99.8	THF	RCI Labscan	RCI Labscan Ltd, Bangkok,	19120112
<i>Ceramic</i>					
Lithium disilicate glass ceramic		LDS	IPS e.max Press	Ivoclar Vivadent, Schaan, Liechtenstein	YY25357

**Table 2 The silane coupling agent, solutions, ceramic, and materials used in the present study and their manufacture**

Materials	Concentrations	Code	Brand	Mfg.	Batch No.
<i>Materials</i>					
Commercial silane coupling agent		CSC	Porcelain liner M	Sun Medical Company, Ltd, Shiga, Japan	SF1
Adhesive agent		A	Single Bond Universal adhesive	3M™ ESPE, MN, USA	881130A
Hydrofluoric acid	9	HF	Porcelain Etch	Ultradent Products Inc, UT, USA	BKCWM
Flowable composite resin			Filtek™ Supreme Flowable restorative	3M™ ESPE, MN, USA	NC9309

## **Part I: The various concentrations of ESC and thermocycling challenge**

### **1.1 The specimens preparation**

The LDS specimens (IPS e.max Press, Ivoclar Vivadent, Schaan, Leichtenstein) were prepared by the lost-wax technique (Figure 2) and cut into cylindrical shape (13.0 mm in diameter and 2.0 mm in thickness) (Figure 3) using a low-speed diamond saw (Isomet<sup>®</sup> 5000, BUEHLER Ltd., IL, USA). (Figure 4) with a speed of 1,500 rpm and feed rate of 1.5 mm/min.

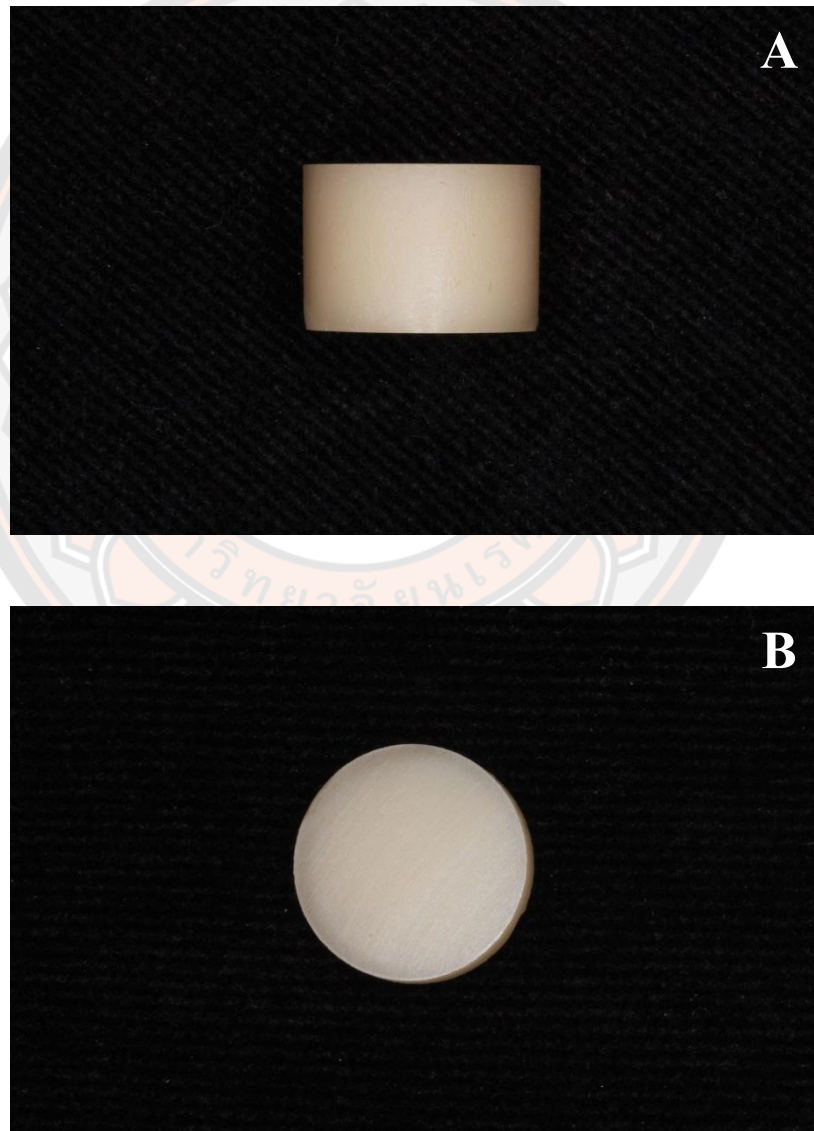


**Figure 2 The LDS specimens (A: the lateral view, B: the top view).**

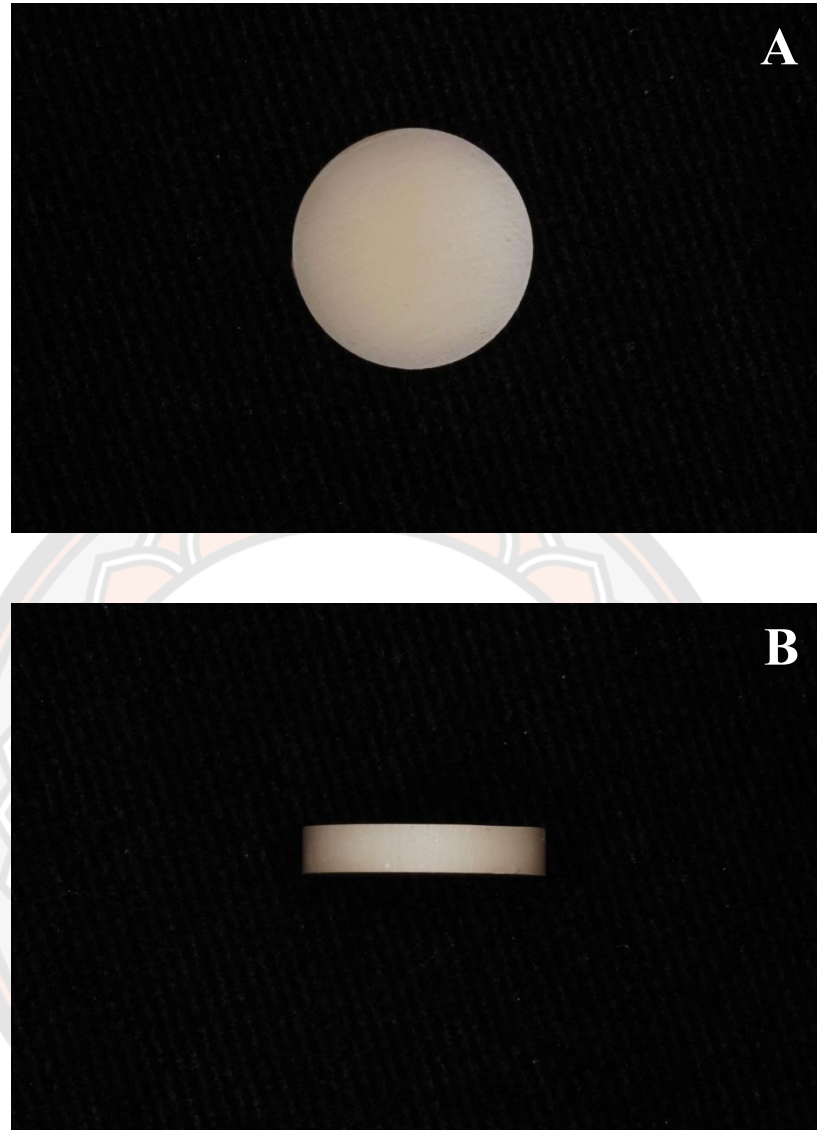


**Figure 3 .The LDS specimens were cut into 13.0 mm in diameter and 2.0 mm in thickness (A: the top view, B: the lateral view).**



**Figure 4 The low-speed diamond saw.**

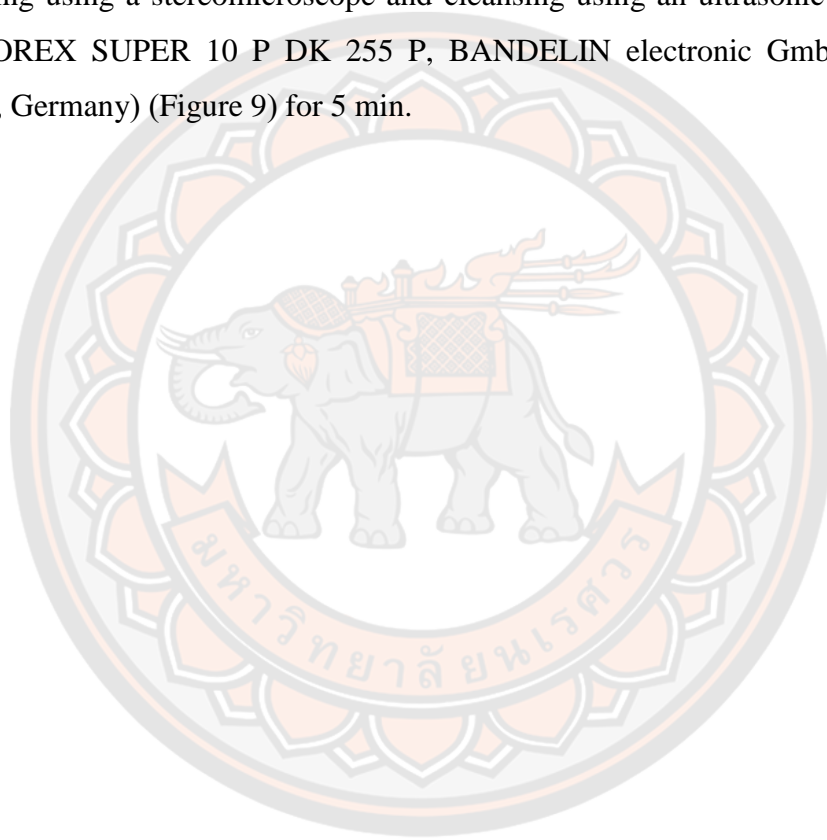
The surface of the LDS specimen was observed under six magnifications using a stereomicroscope (Olympus SZX2-ILLT, Olympus Corporation, Tokyo, Japan) (Figure 5) to determine the cracks on the surface of the LDS specimens. The cracked specimens were then excluded (Figure 6).



**Figure 5 The stereomicroscope.**



Ninety-eight LDS specimens were placed into a cylindrical polyvinylchloride mold (20.0 in diameter and 15.0 mm in thickness) and fixed with auto-polymerized acrylic resin (Fast Curing Custom Tray Acrylic Resin; Instant Tray Mix, Lang dental manufacturing company, IL, USA) (Figure 7). The LDS specimens were polished with wet silicon carbide papers #800, #1000, and #1200 using a polishing machine (Twin variable-speed grinder polisher Phönix Beta 601990, BUEHLER Ltd., IL, USA). (Figure 8). The cracked surface of the LDS specimens was determined after polishing using a stereomicroscope and cleansing using an ultrasonic cleaner device (SONOREX SUPER 10 P DK 255 P, BANDELIN electronic GmbH & Co. KG, Berlin, Germany) (Figure 9) for 5 min.



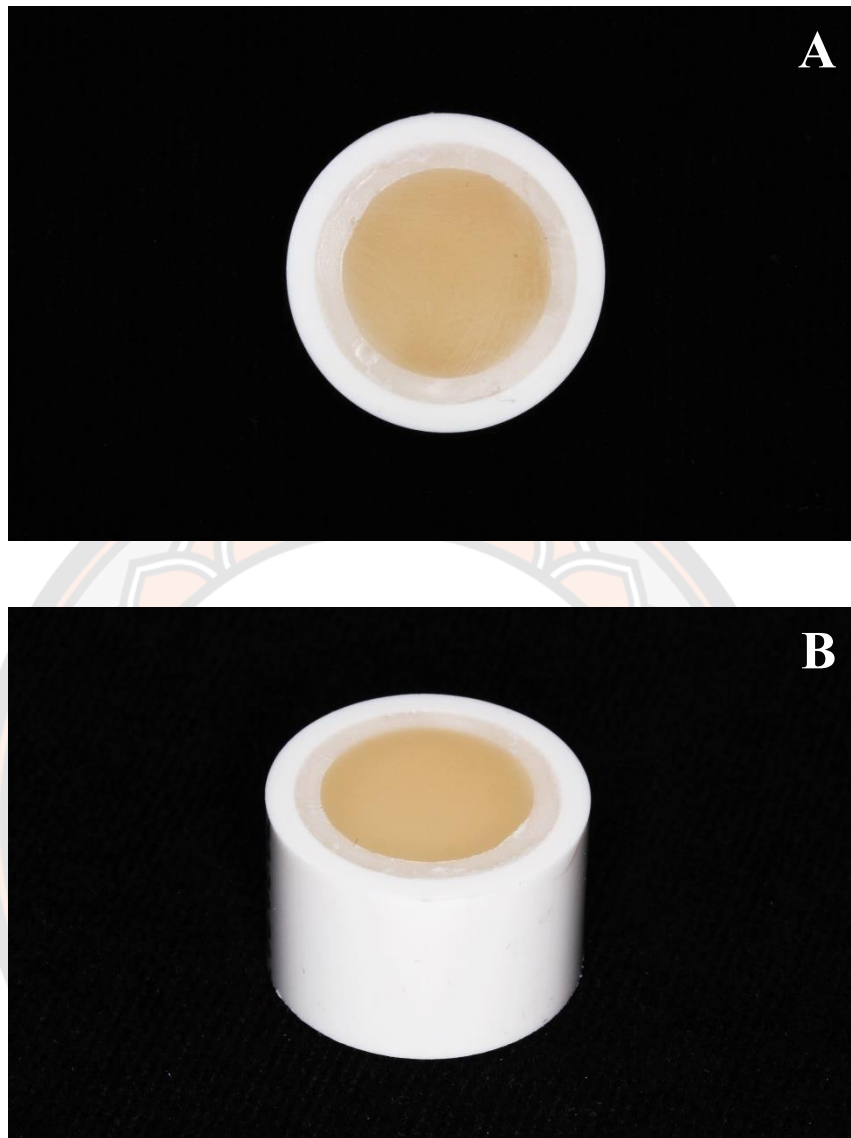


**Figure 7** The 2 millimeter-thickness of LDS specimens were placed into the polyvinylchloride cylindrical mold (20.0x15.0 mm) with auto-polymerized acrylic resin (A: the top view, B: the lateral view).



**Figure 8 The polishing machine.**



**Figure 9 An ultrasonic cleaner device.**

After polishing with wet silicon carbide papers, the surface roughness (Ra) was measured using an atomic force microscope (Nanosurf C3000, Nanosurf Inc., Liestal, Switzerland) (Figure 10) and calculated using software (C3000 Control Software Version 3.5, Nanosurf Inc., Liestal, Switzerland). In all the groups, the Ra values were calculated using One-way analysis of variance (ANOVA). The insignificant differences in the Ra values in all the groups were considered into the experimental specimens. The surface treatment area of LDS specimen's surface was located at the center of the specimen with 5.0 mm in diameter hole of double-side adhesive tape (Scotch® Professional Grade Vinyl Electrical Tape Super 88, 3M ESPE, MN, USA) (Figure 11).



**Figure 10** An atomic force microscopy.

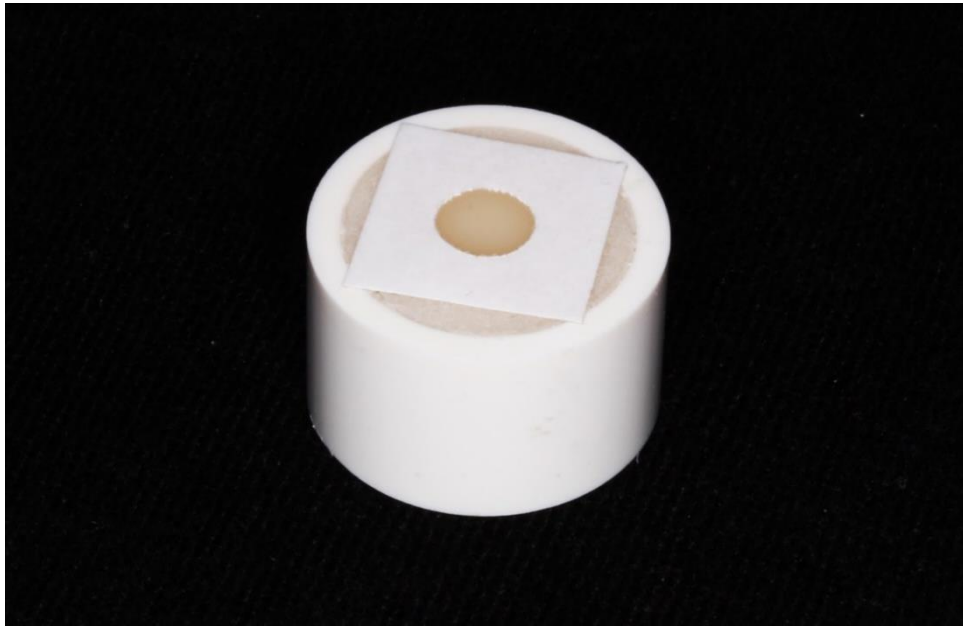


**Figure 11 A double-sided adhesive tape with a 5 millimeter-diameter hole was placed on the LDS specimens.**

Herein, 98 LDS specimens were randomly divided into two conditions: non-thermocycling and thermocycling. Each condition group was divided into seven groups ( $n=7$ ), i.e., 5 groups of various concentrations of ESC, including 1%, 3%, 6%, 9%, and 12% (v/v), and two control groups, which were non-silanization (NS) and commercial silane coupling agent (CSC). The varying concentrations of ESC were prepared by the silanization process as follows (Table 3).

**Table 3 The experimental groups in this study**

No	Surface treatment	Group
1	Adhesive agent	NS
2	HF + Porcelain liner M + Adhesive agent	CSC
3	HF + 1% (v/v) silane coupling + Adhesive agent	1% ESC
4	HF + 3% (v/v) silane coupling + Adhesive agent	3% ESC
5	HF + 6% (v/v) silane coupling + Adhesive agent	6% ESC
6	HF + 9% (v/v) silane coupling + Adhesive agent	9% ESC
7	HF + 12% (v/v) silane coupling + Adhesive agent	12% ESC

\* HF is Hydrofluoric acid

### 1.2 Silanization process

The 99.9% (v/v) of ethanol (ETH; RCI Labscan Ltd, Bangkok, Thailand) (Figure 12) was diluted to 70% ETH with deionized water at room temperature (RT) ( $23\pm 2^{\circ}\text{C}$ ). The mentioned concentrations of ESC were prepared by mixing  $\gamma$ -methacryloxypropyltrimethoxysilane (Sigma-Aldrich<sup>®</sup> Pte Ltd., Mo, USA) (Figure 13) with ETH (Table 4). The reagents were hydrolyzed using a magnetic stirrer (OkWell 6 Ch Stirrer, Progress Technical Co., Ltd., Bangkok, Thailand) (Figure 14) for 5 min.

**Table 4 The amount of ETH and MPS in each ESC group**

No	Amount of 70% (v/v) ETH	Amount of 98% (v/v) MPS	Concentration of ESC (%v/v)
1	19.8	0.2	1% ESC
2	19.4	0.6	3% ESC
3	18.8	1.2	6% ESC
4	18.2	1.8	9% ESC
5	17.6	2.4	12% ESC



Figure 12 The 99.9% (v/v) ETH.



Figure 13 The 98% (v/v) of MPS.



**Figure 14 A: The magnetic stirrer, B: The hydrolysis process of ESC was performed using the magnetic stirrer.**

### 1.3 Surface treatment

#### 1.3.1 HF

The surface of the LDS specimen was conditioned with 9% HF (Ultradent® Porcelain Etch, Ultradent Products Inc., UT, USA) for 90 s in accordance with the manufacturer's instructions (Figure 15). The LDS specimens were rinsed with deionized water for 15 s and dried with an air blow using a triple syringe (Figure 16).

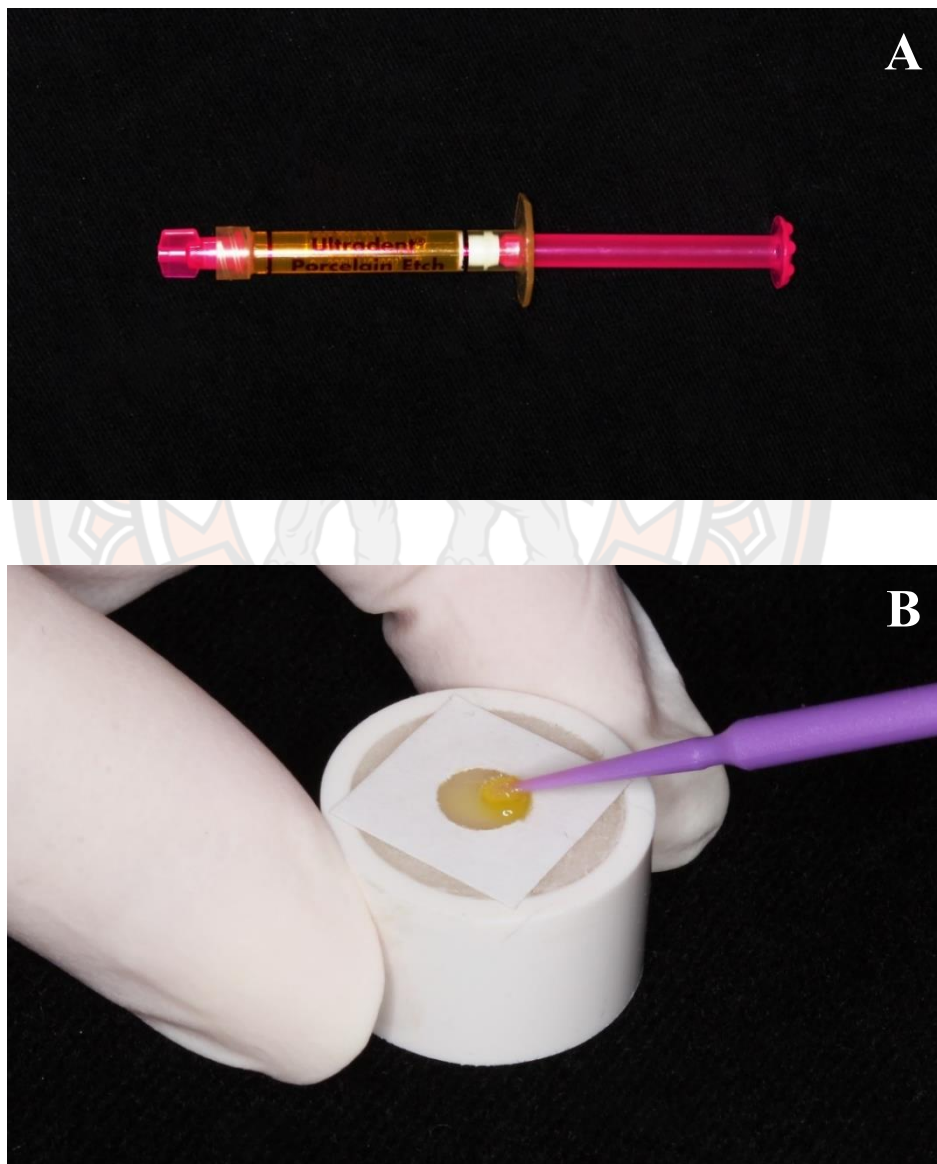


**Figure 15 A: The 9% hydrofluoric acid, B: The surface treatment of LDS specimens with 9% hydrofluoric acid.**

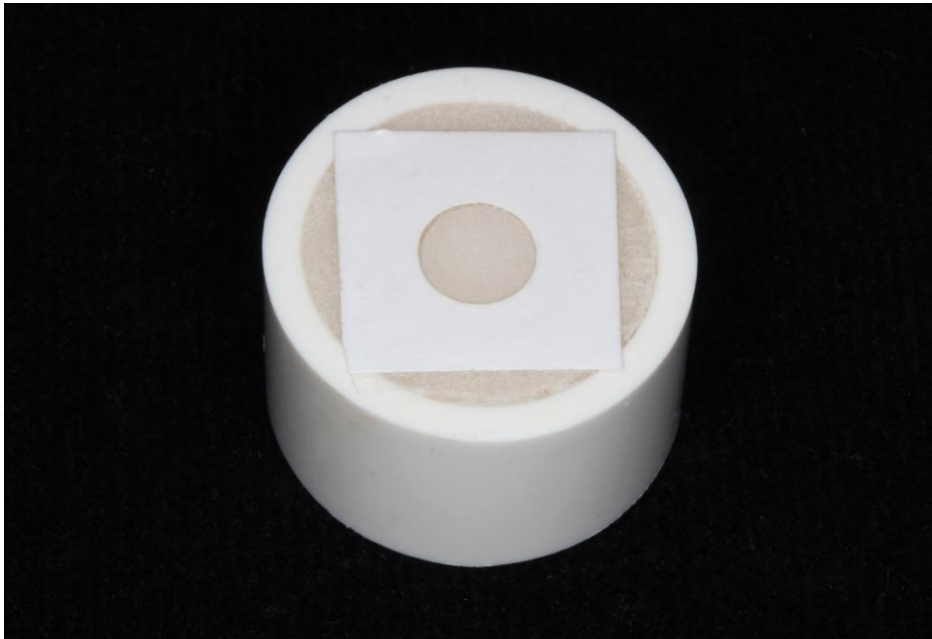


**Figure 16** The bonding area of LDS specimens after surface treatment with 9% hydrofluoric acid.

### 1.3.2 ESC

Thereafter, 50  $\mu\text{L}$  of each concentration of silane coupling agent was applied to the bonding area of the LDS specimens using a micropipette (Pipetman<sup>®</sup> Classic, Gilson Inc., Middleton, USA) (Figure 17) and dried at RT for 1 min.

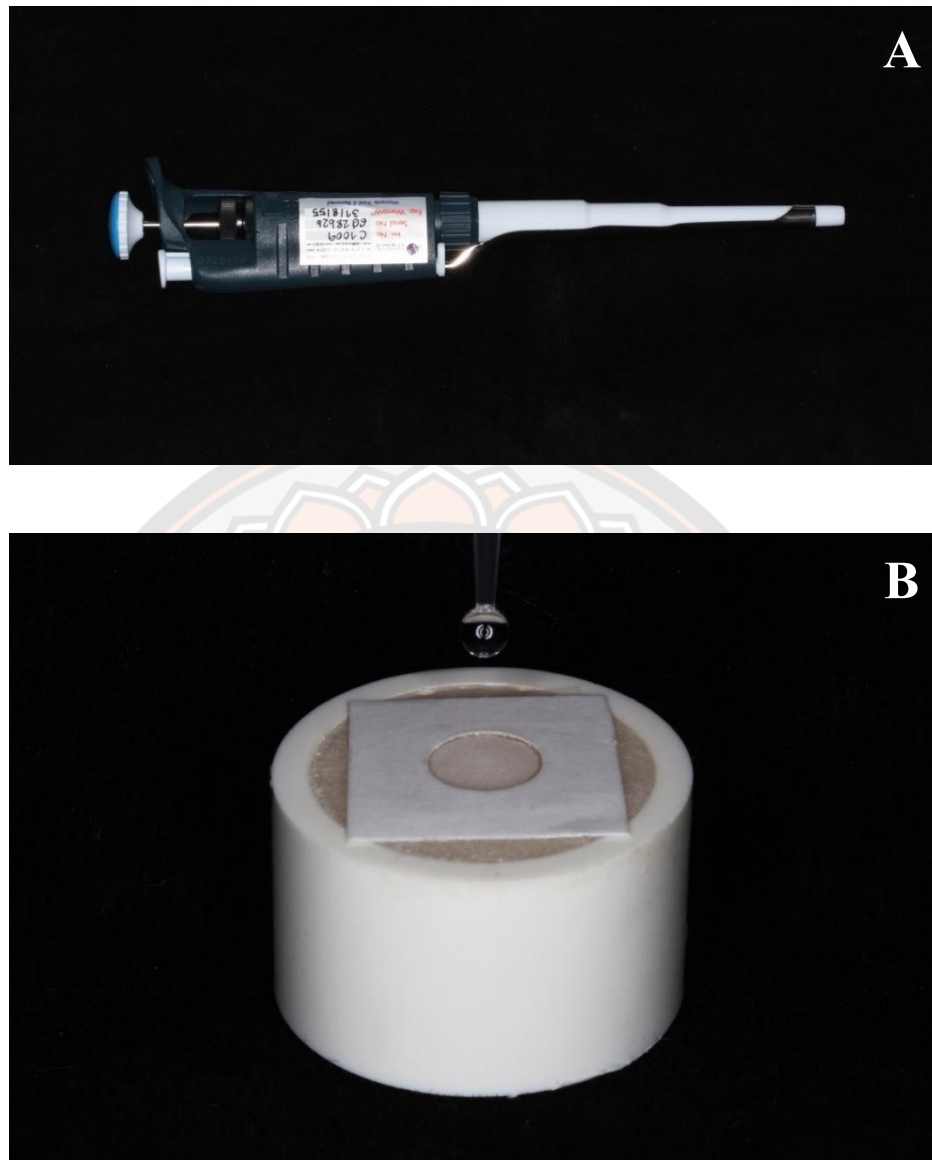


**Figure 17 A: The micropipette, B: The application of the 50 microliters of CSC and each concentration of ESC on the bonding area of LDS specimens use by micropipette.**

### 1.3.3 Commercial silane coupling agent

The Porcelain liner M (pre-hydrolyzed silane coupling agent; Sun Medical Company Ltd., Shiga, Japan) (Figure 18) was used as a CSC agent. Herein, 14 LDS specimens from the CSC group were treated with Porcelain liner M in accordance with the manufacturer's instructions. In each group, they were divided into two conditions: non-thermocycling and thermocycling conditions.



**Figure 18** The commercial silane coupling agent.

### 1.4 Adhesive agent

The adhesive agent (Single Bond Universal adhesive, 3M ESPE, MN, USA) (Figure 19) was applied to the bonding area of the LDS specimens and dried to create a thin film of adhesive layer. The adhesive layer was cured with an LED light-curing unit (Elipar™ S10 LED Curing Light; intensity 1,200 mW/cm<sup>2</sup>, 3M ESPE, MN, USA) (Figure 20) for 10 s in accordance with the manufacturer's instructions. The curing light output was tested after finishing every 7 specimens to check for uniformity of light output using a radiometer.



**Figure 19** The adhesive agent.



**Figure 20** The LED light-curing unit.

### 1.5 Composite resin

The polyvinylchloride tube (5.0 millimeter-diameter and 3.0 millimeter-height) was placed over the bonding area and acts as a mold for composite resin (figure 21). The flowable composite resin (Filtek™ Supreme Flowable restorative, 3M ESPE, MN, USA) (Figure 22) was injected into a polyvinylchloride mold (5.0 mm in diameter and 3.0 mm in height) over the surface treatment area, covered with celluloid strip, and then light activated on each side with five overlapping for 20 s each using LED light-curing unit for 20 s.

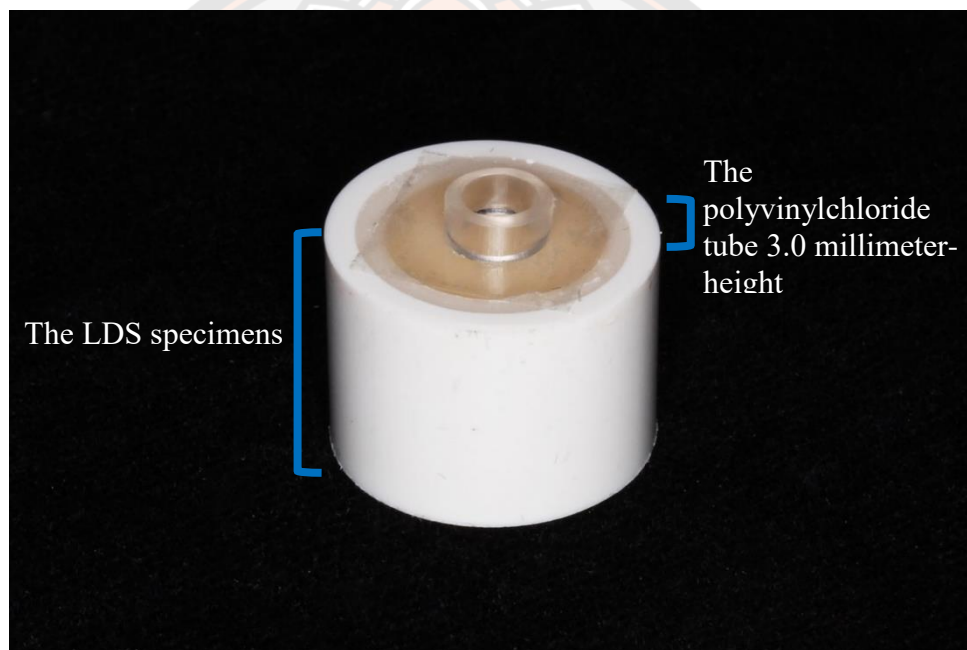


**Figure 21** The 3.0 millimeter-height of polyvinylchloride tube was placed over the bonding area and act as the composite resin mold.



**Figure 22 The flowable composite resin.**

### **1.6 Non-thermocycling and thermocycling challenge**

All the LDS specimens were stored in a dry electronic cabinet (EUREKA Dry Tech DX-126 Auto Dry Box, Taiwan Dry Tech Corporation, Taipei City, Taiwan) (Figure 23) at 37°C for 24 h. Seven LDS specimens in each group were randomly selected for thermocycling conditions. Thermocycling was performed by immersing the specimens in 5°C and 55°C deionized water for 30 s for 5,000 cycles of dwelling time [33, 34] using a thermocycling machine (Thermocycler THE 1200, SD Mechatronik GmbH, Bavaria, Germany) (Figure 24).



**Figure 23 The dry electronic cabinet.**



**Figure 24 The thermocycling apparatus.**

### 1.7 Shear bond strength test

The shear bond strength test was performed using a universal testing machine (ElectroPlus™ E1000, Instron®, MA, USA) (Figure 25) at a crossed-head speed of 0.5 mm/min. The specimens were fixed on a shear bond jig to locate a chisel-shaped rod of the load cell parallel to the bonding interface (Figure 26). The shear bond strength was calculated using software (Bluehill® Universal Materials Testing Software, Instron®, MN, US) with the following equation:

$$\tau = F/A \text{ (N/mm}^2\text{)},$$

where  $\tau$  is the shear stress (N/mm<sup>2</sup>),  $F$  is the applied force (N), and  $A$  is the cross-sectional area of the material with area parallel to the applied force vector (mm<sup>2</sup>).

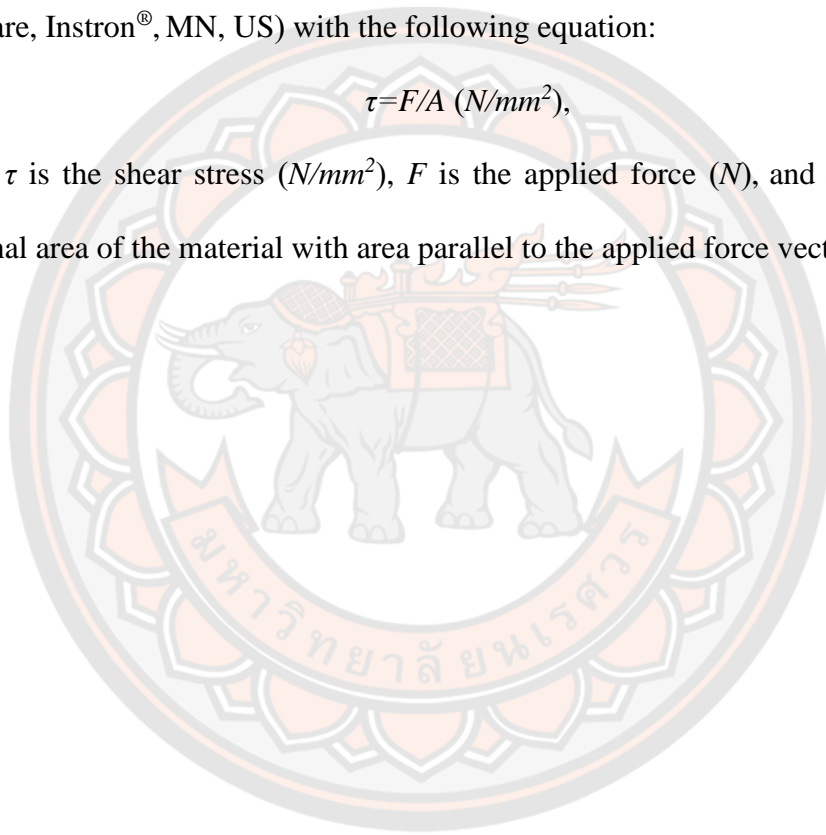




**Figure 25 The universal testing machines.**

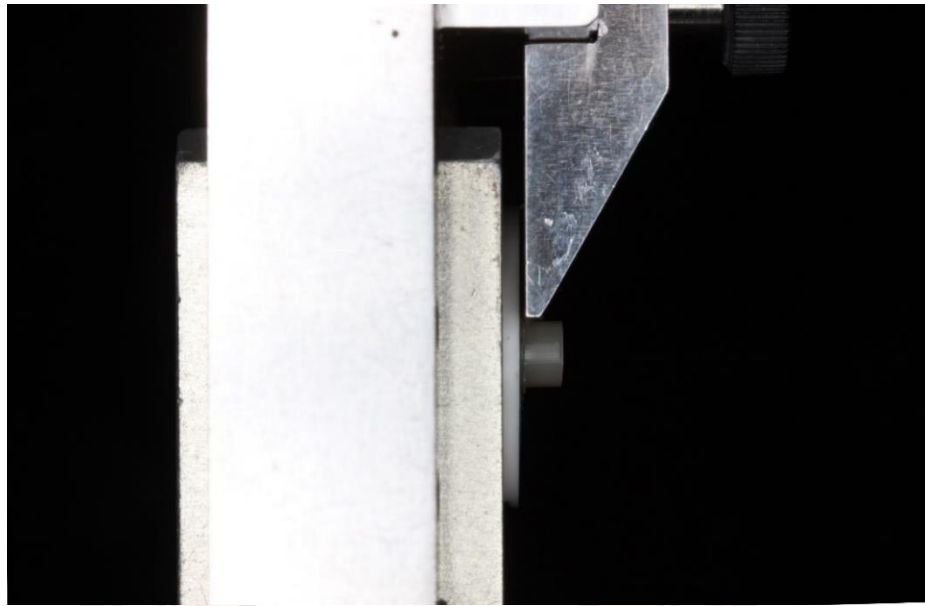


**Figure 26 Set-up the LDS specimens for shear bond test.**

### **1.8 Mode of failure analysis**

The fracture surface characteristics of all experimental LDS specimens after shear bond strength test in part I were examined under 6 magnification of stereomicroscope. The mode of failures of all experimental LDS specimens in non-thermocycling and thermocycling conditions were categorized into 3 characteristics; adhesive failure, cohesive failure, and mixed failure mode (Figure 27). According to the LDS specimens in the mixed failure mode, the composite resin remnants were recorded using Image J software (Image J 1.53k, National Institutes of Health (NIH), Maryland, USA). The mean percentage composite resin remnants were calculated as follows:

$$\text{The mean percentage composite resin remnants} = \frac{\text{The composite resin remnants}}{\text{The total bonding area of LDS specimens}} \times 100$$

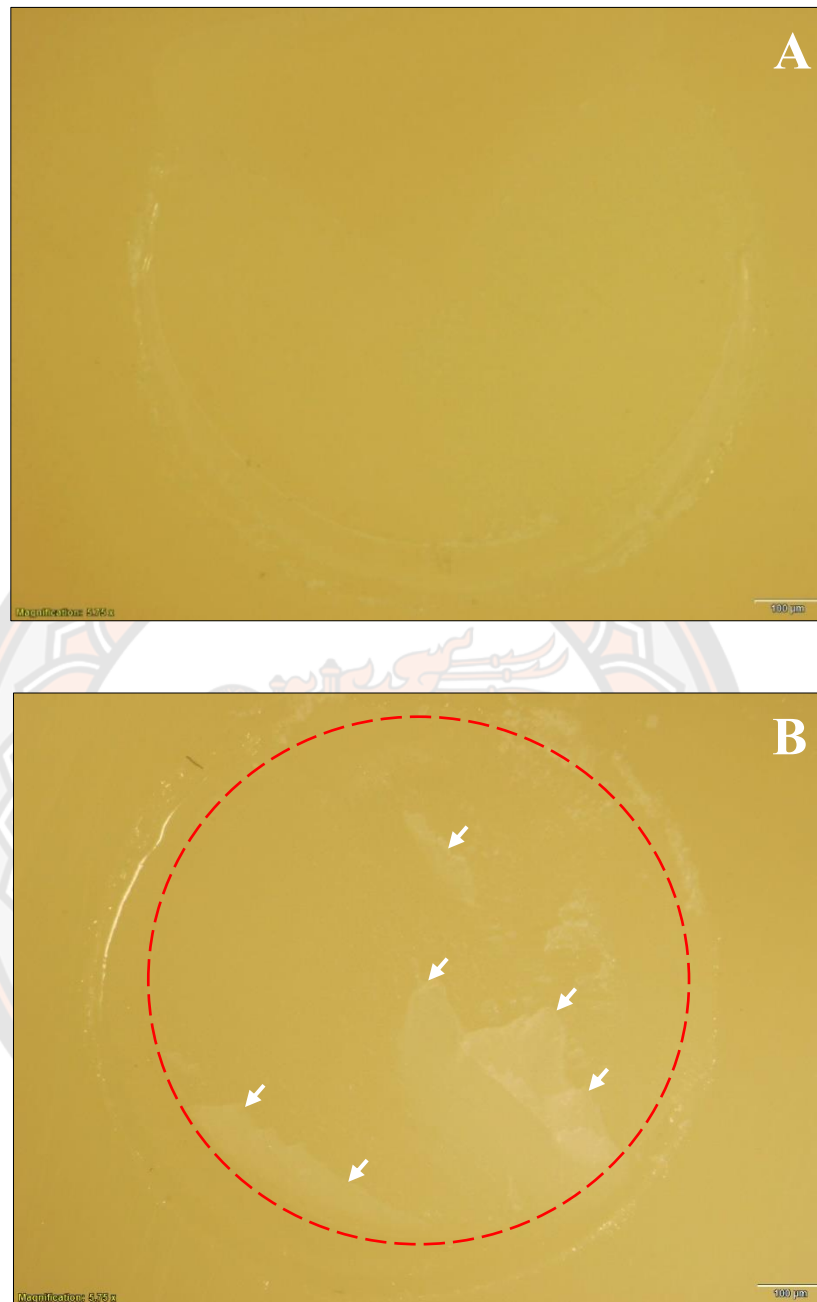


**Figure 27** The fracture surface of LDS specimens after shear bond strength test under the stereomicroscope, **A:** The adhesive failure, **B:** the mixed failure mode, Red dash circle represent bonding area, White arrow represent composite resin remnants

## **1.9 Scanning electron microscopy (SEM)**

The fractured surfaces of LDS specimens after the shear bond strength test were observed using a SEM (Leo 1455VP, Carl Zeiss Microscopy GmbH, Jena, Germany). After the shear bond strength test, the fractured surfaces of the LDS specimens were coated with a thin layer of gold. The primary electron beam energy was operated at 20 keV for each specimen.

### **Part II: The shelf life of hydrolyzed silane coupling agent.**

#### **1 Shelf life of hydrolyzed silane coupling agent.**

Based on the shear bond strength test results in Part I, 6% ESC group showed the highest shear bond strength and was therefore selected to evaluate the shelf life of the hydrolyzed silane coupling agent. The 6% hydrolyzed ESC was stored in a polypropylene tube which was wrap by aluminum foil and kept in a dry electronic cabinet at RT. In addition, the 6% hydrolyzed ESC was stored for at least 32 days to analyze the effect of the shelf life of hydrolyzed silane after the silanization process through this Part II method.

Herein, 49 LDS specimens were divided into seven groups ( $n=7$ ) at 0, 1, 2, 4, 8, 16, and 32 days after the silanization process. The procedures of the LDS specimen preparation, silanization process, adhesive agent, composite resin, thermocycling condition, and shear bond strength test were similar to those of Part I.

### **Part III: The Elemental analysis.**

#### **1 Elemental analysis**

To clarify the effectiveness of silane coupling agent deposition on the LDS surface after silanization, the LDS specimens were washed with an excess silane coupling agent with tetrahydrofuran (THF; RCI Labscan Ltd, Bangkok, Thailand) (Figure 28). Eleven LDS specimens were prepared for the silanization process with 1%, 3%, 6%, 9%, and 12% ESC groups following the above-mentioned procedures. In each ESC group, the specimens were divided into two conditions: washed THF and unwashed THF. The non-silanized surface of LDS specimen was treated with 9% HF and analyzed as a reference (Etched LDS group).

In the washed THF condition, the homocondensation and physisorbed layers of the silane coupling agent were removed [38, 39]. The washing procedure was repeated until the THF supernatant showed only an absorbance peak at 250 nm using a spectrophotometer (SpectraMax<sup>®</sup> M3 Microplate Reader, Molecular Devices LLC, California, USA) (Figure 29). This procedure indicated that it was possible to completely remove the homocondensation and physisorbed layer from the surface of the LDS specimen.

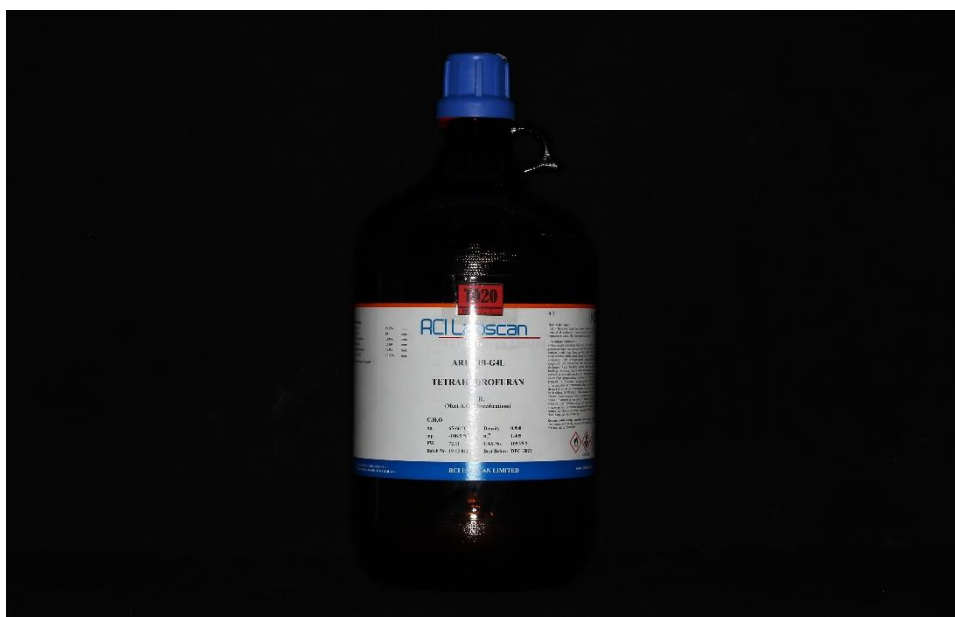


**Figure 28** The tetrahydrofuran.



**Figure 29** The spectrophotometer.

Energy dispersive X-ray spectroscopy (EDS; S-3400N-II, Hitachi High-Technologies Corporation, Tokyo, Japan) was used to evaluate the qualitative and quantitative characteristics of the elements on the surface of the specimens. A thin layer of gold was coated onto the surface of the LDS specimens. The primary electron beam energy was operated at 20 keV for each specimen. Three areas of  $0.25 \times 0.18$  mm, which were the center of the specimen, were examined. The non-silanized surface of the LDS specimen was treated with 9% HF and analyzed as a reference (Etched LDS group). EDS analysis can detect carbon (C), oxygen (O), and silicon (Si) atoms on the silanized LDS surface. Si and O atoms can be detected on the non-silanized and silanized surfaces of the LDS specimens. Therefore, the C atom is the appropriate element to demonstrate that the silane coupling agent reacted on the LDS surface.

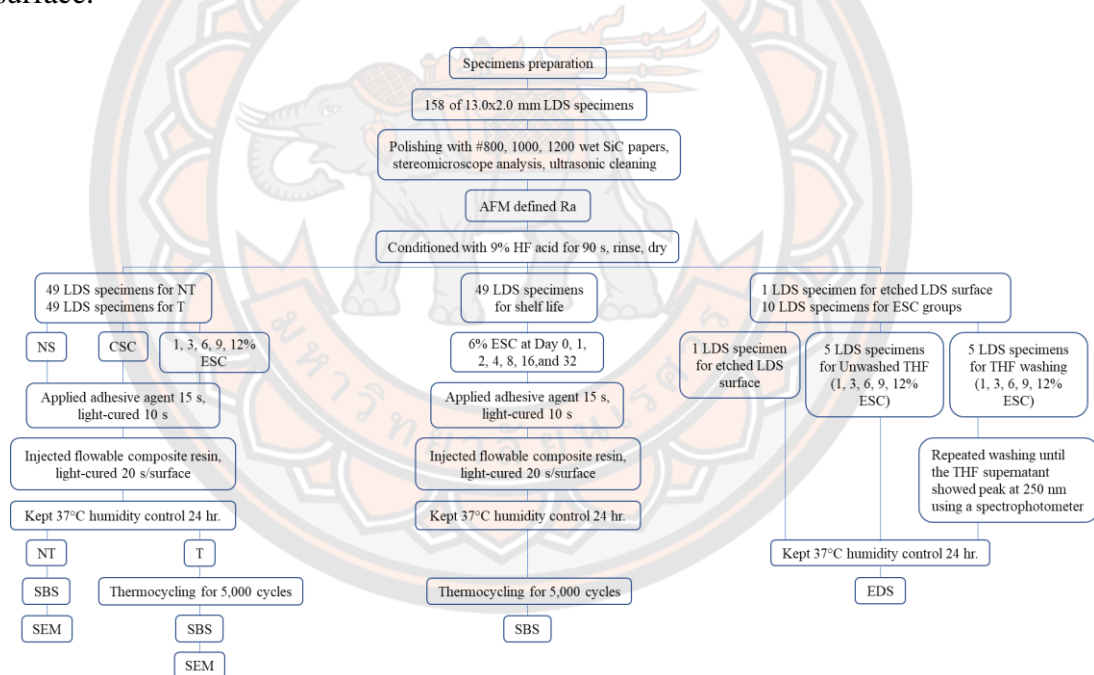


**Figure 30** Experimental procedure schematic.

**Statistical analysis**

The shear bond strength of various concentrations of the silane coupling agent under non-thermocycling and thermocycling conditions was analyzed using Two-way ANOVA, followed by Tukey's *post-hoc* comparison (SPSS version20, IBM, Armonk, NY, USA). The shear bond strength of various concentrations and shelf life of the hydrolyzed silane were determined using One-way ANOVA and Tukey's *post-hoc* comparison. The significance level was set at  $\alpha=0.05$ .



## CHAPTER V

### RESULTS

#### 1 The surface roughness (Ra) of lithium disilicate glass ceramic

The surface roughness (Ra) of the LDS specimens after polished was evaluated using atomic force microscopy. One-way ANOVA revealed insignificantly different Ra values among groups. Therefore, Ra value among groups were accepted. The average Ra value were shown in Table.5.

**Table 5 The means and standard deviations of the Ra value**

Group	Mean of surface roughness (nm)(SD)
NS	14.6 (3.8) <sup>a</sup>
CSC	14.7 (3.8) <sup>a</sup>
1% ESC	14.8 (3.9) <sup>a</sup>
3% ESC	14.8 (3.9) <sup>a</sup>
6% ESC	15.0 (3.9) <sup>a</sup>
9% ESC	15.1 (3.9) <sup>a</sup>
12% ESC	15.2 (3.9) <sup>a</sup>

% (v/v)

Mean values ( $n=7$ ) and standard deviations in parentheses.

\*Superscript letters denoted with same letter are not significantly different ( $p > 0.05$ ).

#### 2 The various concentration of ESC and thermocycling challenge

Two-way ANOVA showed that the interaction of the two main factors between the silane coupling agent concentrations and the thermocycling challenge was insignificant. Nevertheless, the effect of each factor was statistically significant among the groups. Therefore, One-way ANOVA and Tukey's HSD tests were performed to compare all the conditions. The means and standard deviations of the

shear bond strength under non-thermocycling and thermocycling conditions are shown in Table 6.

**Table 6 The means and standard deviations of shear bond strength in non-thermocycling and thermocycling conditions**

Surface treatment	Shear bond strength (MPa)	
	Non-thermocycling	Thermocycling
NS	7.3 (1.0) <sup>d</sup>	1.8 (0.6) <sup>D</sup>
CSC	18.0 (2.3) <sup>c</sup>	13.8 (2.0) <sup>B,C</sup>
1% ESC	20.5 (4.5) <sup>b,c</sup>	14.5 (2.3) <sup>B,C</sup>
3% ESC	23.2 (2.7) <sup>a,b</sup>	15.6 (2.3) <sup>A,B</sup>
6% ESC	26.3 (2.6) <sup>a</sup>	18.2 (1.8) <sup>A</sup>
9% ESC	22.8 (3.3) <sup>a,b,c</sup>	15.9 (2.3) <sup>A,B</sup>
12% ESC	22.1 (3.4) <sup>a,b,c</sup>	12.0 (3.0) <sup>C</sup>

% (v/v)

Mean values ( $n=7$ ) and standard deviations in parentheses.

\*Superscript letters denoted with same letter are not significantly different ( $p > 0.05$ ).

The means of the shear bond strength of the NS, CSC, and 1%, 3%, 6%, 9%, and 12% ESC groups with non-thermocycling conditions ranged from 7.3 to 26.3 MPa. One-way ANOVA revealed significant differences between the groups. Tukey's HSD indicated that the means of the shear bond strength of 3%, 6%, 9%, and 12% ESC groups were 23.2, 26.3, 22.8, and 22.1 MPa, respectively, all of which were significantly higher than those of the other groups. The 6% ESC group exhibited the highest shear bond strength. Furthermore, the mean shear bond strength of the NS group was 7.3 MPa, and it revealed significantly lower shear bond strength than that of the CSC and ESC groups.

Under thermocycling conditions, the means of the shear bond strength of the NS, CSC, and 1%, 3%, 6%, 9%, and 12% ESC groups ranged from 1.8 to 18.2 MPa. One-way ANOVA revealed significant differences between the groups. Tukey's HSD indicated that the shear bond strengths of 3%, 6%, and 9% were 15.6, 18.2, and 15.9

MPa, respectively, which were significantly higher than those of the other groups. The 6% ESC group exhibited the highest shear bond strength. The mean shear bond strength of the NS group was 1.8 MPa, which was significantly lower than that of the CSC and ESC groups. Consequently, Two-way ANOVA revealed significant differences between the groups in the non-thermocycling and thermocycling conditions. In other words, the shear bond strength in the non-thermocycling conditions was significantly higher than that in the thermocycling conditions.

### **3 Mode of failure analysis**

After the shear bond strength test, all experimental LDS specimens in Part I were observed under six magnifications using a stereomicroscope to determine the mode of failure (Figure 27). The mode of failure of the experimental LDS specimens under non-thermocycling and thermocycling conditions is shown in Table 7. The mean percentages of composite resin remnants in the 6% ESC group with non-thermocycling and thermocycling conditions were 30.8% and 8.9%, respectively.

**Table 7 Mode of failures and means percentage of composite resin remnants of experimental LDS specimens in non-thermocycling and thermocycling conditions (n=7)**

Surface treatment	Mode of failures							Means of composite resin remnants (%)
	Non-thermocycling			Thermocycling				
	Adhesive	Cohesive	Mixed	Adhesive	Cohesive	Mixed		
	n	n	n	n	n	n		
NS	7	0	0	0	7	0	0	0
CSC	6	0	1	12.9	5	0	2	4.9
1% ESC	3	0	4	13.5	3	0	4	5.0
3% ESC	2	0	5	26.5	3	0	4	5.1
6% ESC	0	0	7	30.8	0	0	7	8.9
9% ESC	2	0	5	14.7	3	0	4	2.0
12% ESC	4	0	3	10.0	5	0	2	1.9

#### 4 The shelf life of hydrolyzed silane coupling agent.

The means and standard deviations of the shear bond strength values of 0, 1, 2, 4, 8, 16, and 32 days after hydrolyzing 6% ESC are summarized in Table 8. The values ranged from 13.7 to 18.2 MPa. One-way ANOVA revealed significant differences between groups. The means of the shear bond strength at 0 and 1 d after hydrolyzing the 6% ESC group were 18.2 MPa and Tukey's HSD was significantly higher than those of the other groups. Moreover, the shear bond strength of the hydrolyzed 6% ESC gradually decreased over time. The shear bond strength at 32 days after hydrolyzing the 6% ESC group was 13.7 MPa, which was significantly lower than that of the other groups.

**Table 8 The means and standard deviations of the shear bond strength of hydrolyzed 6% ESC**

Day	Shear bond strength (MPa)
0	18.2 (1.8) <sup>A</sup>
1	18.2 (2.3) <sup>A</sup>
2	17.1 (2.8) <sup>A, B</sup>
4	16.4 (2.6) <sup>A, B</sup>
8	14.6 (1.6) <sup>A, B</sup>
16	14.6 (1.6) <sup>A, B</sup>
32	13.7 (2.5) <sup>B</sup>

Mean values ( $n=7$ ) and standard deviations in parentheses.

\*Superscript letters denoted with same letter are not significantly different ( $p > 0.05$ ).

## 5 The elemental analysis

The atomic percentages of C atoms on the surface of the LDS specimens in unwashed THF and washed THF conditions are shown in Figure 31. After silanization in the unwashed THF condition, the atomic percentage of C atoms ranged from 0.08 to 7.41. The atomic percentage of C atoms gradually increased and reached the highest value in the 12% ESC group. The atomic percentage of C atoms after THF washing ranged from 1.38 to 2.88 and gradually increased from 1% in the ESC group and reached a plateau in the 6% ESC group.

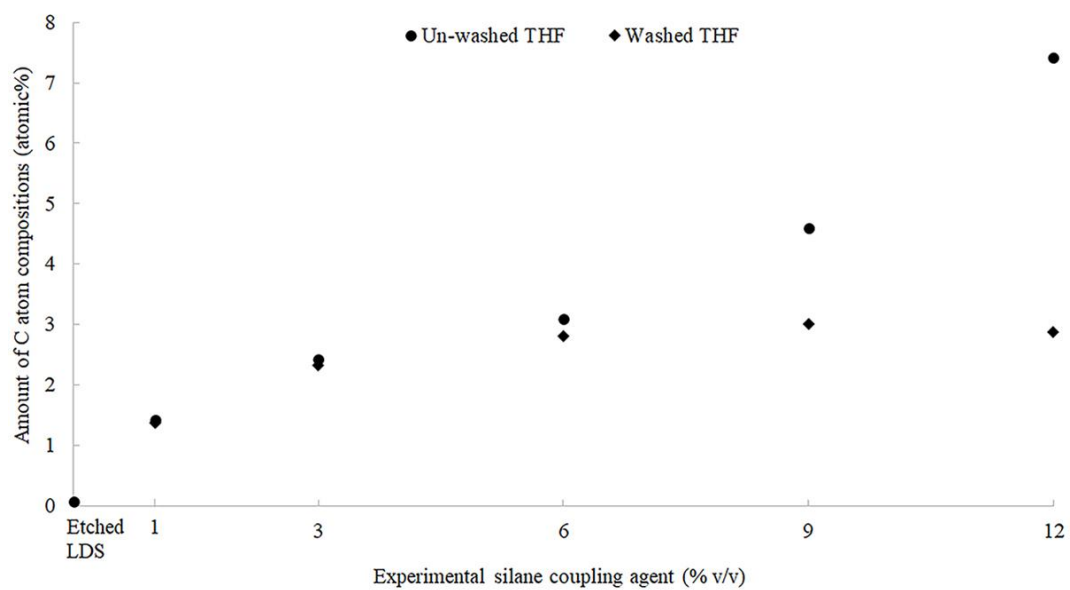


**Figure 31** The atomic percentages of C atom on the surface of LDS specimens in un-washed THF and washed THF conditions

## CHAPTER VI

### DISCUSSION

This study evaluated the effect of different concentrations of silane coupling agent and thermocycling challenge on the shear bond strength between LDS and composite resin. Two-way ANOVA revealed no significant difference in the two factors between the concentrations of silane coupling agents and thermocycling challenge. Therefore, the null hypothesis that there would be no significant difference between the various concentrations of silane coupling agent and thermocycling challenge on the shear bond strength between LDS and composite resin was accepted. Nevertheless, each factor of the silane coupling agent and thermocycling challenge revealed significant differences among the groups. One-way ANOVA and Tukey's HSD were performed to compare all the conditions.

In this study, the effects of different concentrations of the silane coupling agent on the shear bond strength between LDS and composite resin were determined. The results showed that the shear bond strength in the non-thermocycling conditions of the NS group (7.28 MPa) was significantly lower than that of the other groups. The 3%, 6%, 9%, and 12% ESC groups had a significantly higher shear bond strength than the other groups, suggesting that the surface treatment on the LDS surface was a crucial factor in creating a higher shear bond strength between the LDS surface and composite resin. Surface treatment with HF on the LDS surface could remove the glass matrix on the LDS surface, allowing the silane coupling agent and adhesive agent to better penetrate the HF-treated LDS surface, which increased the micromechanical retention and resulted in a statistically high shear bond strength [3, 40]. The adhesive agent in this study consists of silane coupling agent which was not affected chemical bonds on LDS surface due to their ineffectiveness, instability, the acidic solution in this adhesive agent promoted homocondensation [41-43], and the others in composition of this one-bottle of adhesive agent i.e. Bis-GMA may inhibit the action of silane by interrupting the forming of siloxane bond to the hydroxyl group of ceramic surfaces [43].

The characteristics of the silane layer on the LDS surface can affect the shear bond strength between the LDS and composite resin, which consists of chemisorbed and physisorbed layers [22]. The results of this study showed that 6% ESC groups provided the highest shear bond strength due to the chemisorbed monolayer. The chemisorbed layer created a completely bonded monolayer structure of the silanol group the LDS surface. The lower shear bond strengths of the 1% and 3% ESC groups resulted from a minimal number of silanol groups bonded with the LDS surface, which created an incomplete chemisorbed monolayer. The higher concentrations of MPS in the 9% and 12% ESC groups resulted in decreased shear bond strength. This resulted from the physisorbed layer, which contains weak Van der Waals forces and hydrogen bonds [24]. In addition, after the hydrolysis process, the higher concentrations of silane coupling agent in the 9% and 12% ESC groups tended to cause homocondensation, which created a siloxane bond between the silane molecules, resulting in a minimal number of silanol groups bonded with the LDS surface [10, 27].

The shear bond strength decreased significantly after the thermocycling. The shear bond strengths of the 3%, 6%, and 9% ESC groups were greater than those of the other groups. Previous studies have reported that the moisture of the oral environment induces the hydrolysis of the silane coupling layer, which results in degradation at the adhesive interface [21]. The water molecules entered the silane coupling layers and gradually hydrolyzed the siloxane bonds, resulting in decreased bond strength [44]. In addition, the difference in the thermal expansion coefficients of each material created thermal stress at the interface of the LDS surface, adhesive agent, and composite resin [21]. This study reported that the shear bond strength of hydrolyzed 6% ESC groups gradually decreased over time and was significantly lower than that of the other groups at day 32. These results may be due to the increased level of homocondensation [10, 27].

According to the SEM images of this study, the untreated LDS surface and NS group were similar and showed a smooth surface topography (Figure 32A, 32C). The application of an adhesive agent on a non-etched-LDS surface (NS group) resulted in the lowest shear bond strength. After HF etching, the etched-LDS surface morphology appeared as a typically needle-like crystal. The glassy matrix on the

superficial LDS surface was dissolved and exposed to lithium disilicate crystals. The glassy matrix on the superficial LDS surface was dissolved and exposed the lithium disilicate crystal. (Figure 32B). Surface treatment with a silane coupling agent on the etched-LDS surface promoted chemical bonding. However, the chemisorbed monolayer of the silane coupling agent on the etched-LDS surface was not observed in the SEM topography because of the very thin layer (Figure 33B). The fractured LDS surface covered with an adhesive agent and silane coupling agent layer was frequently observed in the CSC, 1%, and 12% ESC groups under both non-thermocycling and thermocycling conditions (Figure 32D, 32E, 32I, 34B, 34C, 34G). The absence of the remaining composite resin on the fractured LDS surface after the shear bond strength test indicated an inappropriate chemical bond. These results may be due to the incomplete chemisorbed layer of silanol molecules on the LDS in the 1% ESC group. On the other hand, the excess amount of silanol molecules in the 12% ESC group created physisorbed layers and homocondensation (Figure 33C). After the shear bond strength test, the crack that passed through the physisorbed layer resulted in the absence of the remaining composite resin on the fractured LDS surface.

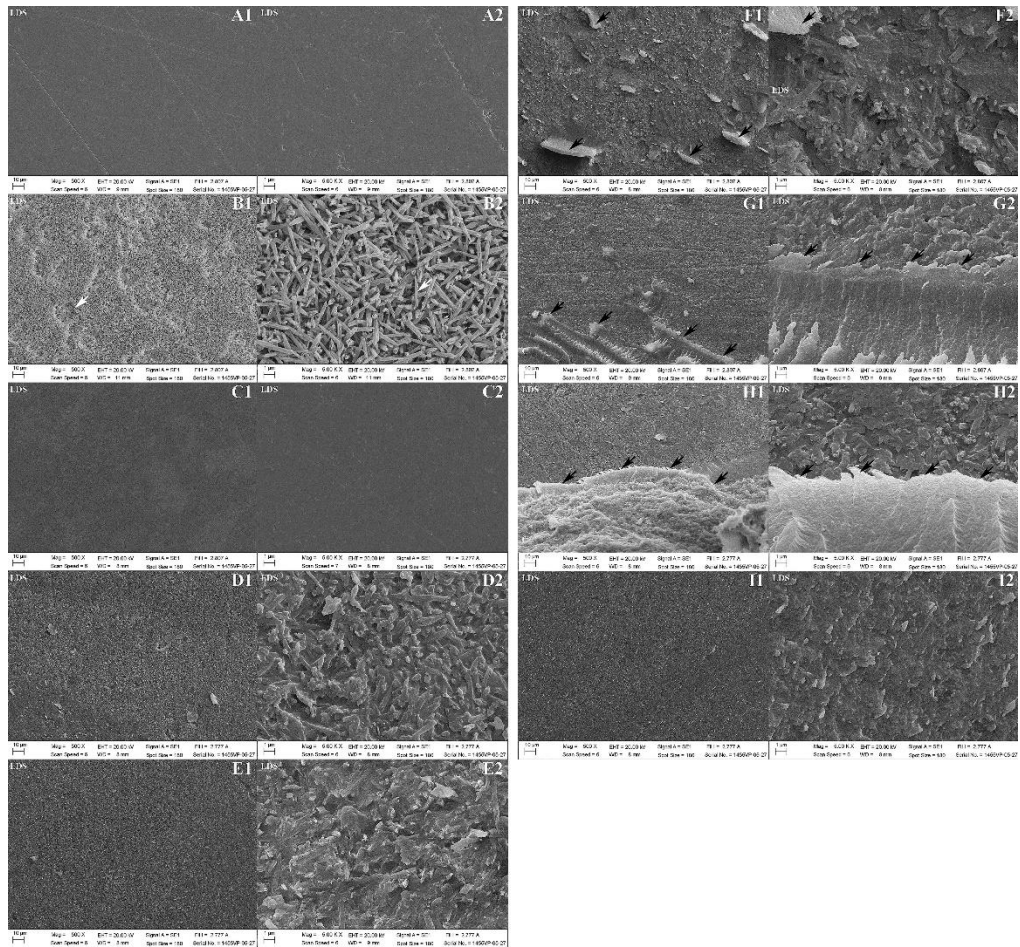


**Figure 32** Representative SEM images of the fractured LDS surfaces in non-thermocycling condition. A1, A2: Non-etched LDS surface, B1: The etched LDS surface. White arrow showed the etched pattern, B2: The etched LDS surface. White arrow showed the lithium disilicate glass particles, C1, C2: Non-silanized LDS surface, D1, D2: The fractured surface of the CSC group, E1, E2: The fractured surface of 1% ESC, F1, F2: The fractured surface of 3% ESC, G1, G2: The fractured surface of 6% ESC, H1, H2: The fractured surface of 9% ESC, I1, I2: The fractured surface of 12% ESC. F1-H2: Black arrows showed the remaining composite resin, 1:500 magnification, 2: 5,000 magnification.

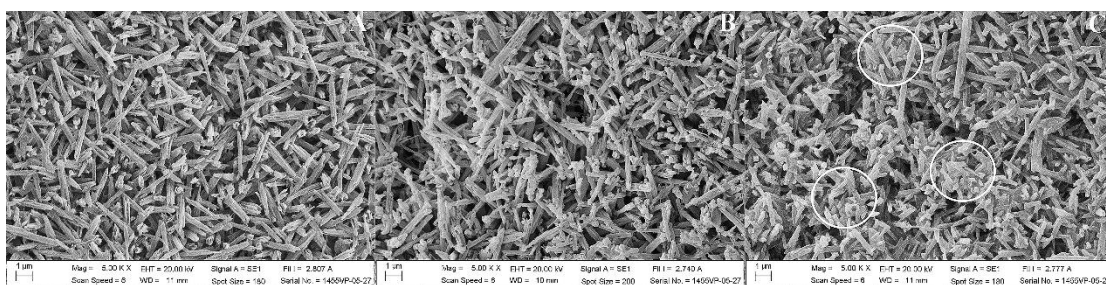


**Figure 33** Representative 5000 magnifications of SEM images on the LDS surfaces. **A:** etched LDS surfaces, **B:** etched and silanized with 6% ESC, **A and B** showed exposed needle-like crystal of LDS, **C:** etched and silanized with 12% ESC. White circle showed the cluster-crystal structure of LDS that was covered with physisorbed layers.

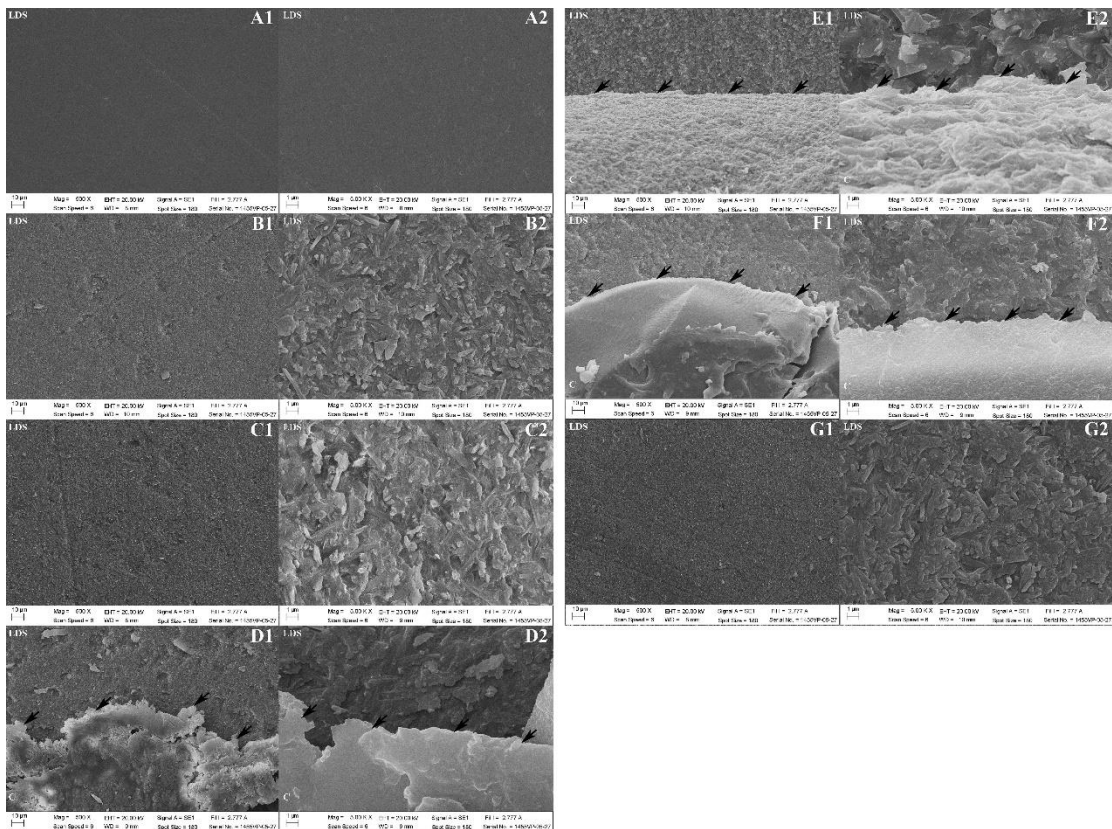


**Figure 34** Representative SEM images of the fractured LDS surfaces in thermocycling condition. A1, A2: Non-silanzed LDS surface, B1, B2: The fractured surface of the CSC group, C1, C2: The fractured surface of 1% ESC, D1, D2: The fractured surface of 3% ESC, E1, E2: The fractured surface of 6% ESC, F1, F2: The fractured surface of 9% ESC, G1, G2: The fractured surface of 12% ESC. D1-F2: Black arrows showed the remaining composite resin, 1: 500 magnification, 2: 5,000 magnification

The fractured surfaces of the 3%, 6%, and 9% ESC groups after the shear bond strength test under non-thermocycling and thermocycling conditions demonstrated a similar trend. The remaining composite resin on the surface of the LDS specimen was observed (Figure 32F-H, 34D-F). This result and the failure modes of the 3%, 6%, and 9% ESC groups were categorized and frequently appeared in the mixed failure mode than in the adhesive failure mode. In addition, all the fracture surfaces of the 6% ESC group in the non-thermocycling and thermocycling conditions demonstrated a mixed failure mode with mean percentages of composite resin remnants of 30.8% and 8.9%, respectively, which showed the highest shear bond strength for each condition.

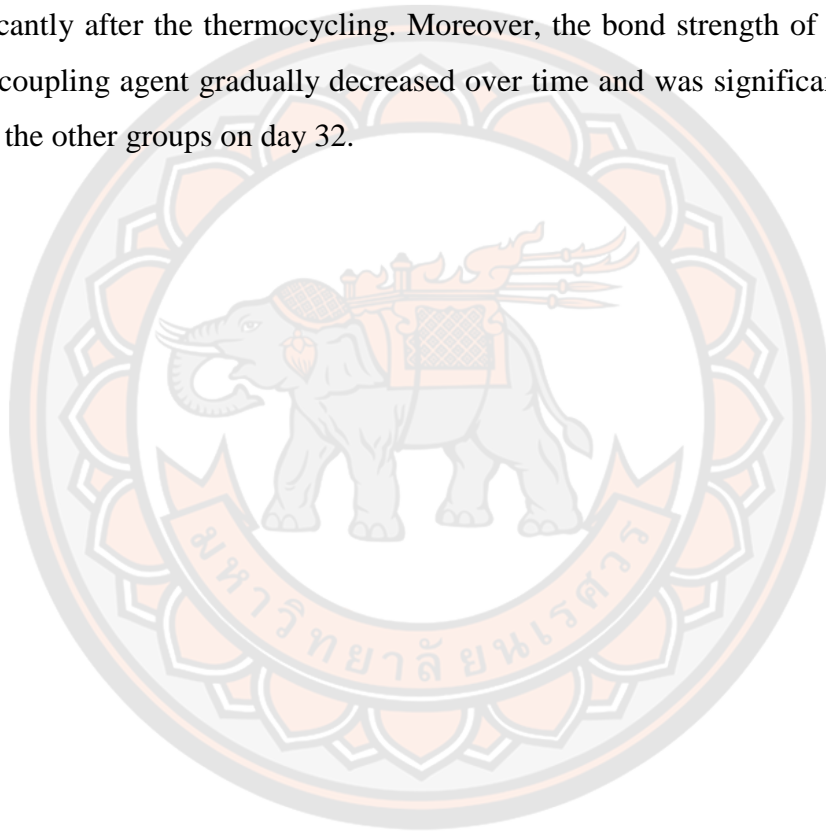
According to the elemental analysis, the chemical molecular structure of the silane coupling agent contains C, Si, and O elements, whereas the LDS consists of Si and O elements. In other words, Si and O were found in both the LDS surface and the silane coupling agent. Therefore, elemental C was the appropriate element to show that the silane coupling agent reacted with the LDS surface.

After silanization in the unwashed THF condition, the lowest C atom appeared in the 1% ESC group. The C atom gradually increased and reached a peak in the 12% ESC group. These results may be due to the increasing amount of C atoms, followed by an increase in the silane coupling agent concentration. In contrast, the number of C atoms after THF washing gradually increased from the 1% ESC group and reached a plateau in the 6% ESC group. The plateau atomic % C of  $\geq 6\%$  ESC in the THF washed groups indicated the complete removal of the physisorbed silane coupling agent by THF washing. Therefore, the 6% ESC group was the optimal concentration for creating a chemisorbed layer on the LDS surface.

## CHAPTER VI

### CONCLUSIONS

Within the limitations of this study, it was concluded that 6% ESC provided the highest shear bond strength. This is due to the optimal chemisorbed monolayer formed along with HF surface etching. The shear bond strength decreased significantly after the thermocycling. Moreover, the bond strength of the hydrolyzed silane coupling agent gradually decreased over time and was significantly lower than that of the other groups on day 32.



## REFERENCES



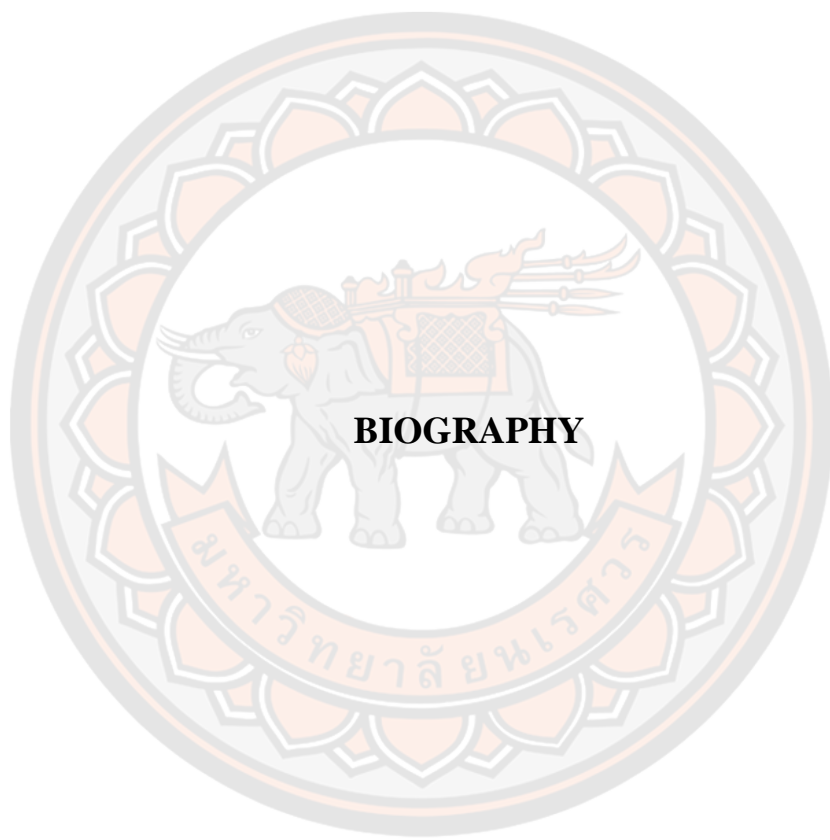
## REFERENCES

- Denry I, Holloway JA. Ceramics for Dental Applications: A Review. *Materials* 2010; 3:351-68.
- Yin L, Stoll R. Ceramics in restorative dentistry. In: Low IM, editor. *Advances in Ceramic Matrix Composites*. 2nd ed. Cambridge: Woodhead publishing Ltd; 2014, p.711-40.
- Soares CJ, Soares PV, Pereira JC, Fonseca RB. Surface treatment protocols in the cementation process of ceramic and laboratory-processed composite restorations: A literature review. *J Esthet Restor Dent* 2005; 17:224-35.
- Asgar K. Casting metals in dentistry: Past-present-future. *Adv Dent Res* 1988; 2:33-43.
- Conrad HJ, Seong WJ, Pesun IJ. Current ceramic materials and systems with clinical recommendation: A systematic review. *J Prosthet Dent* 2007; 98:389-404.
- Cadore-Rodrigues AC, Guilardi LF, Wandscher VF, Pereira GKR, Valandro LF, Rippe MP. Surface treatments of a glass-fiber reinforced composite: Effect on the adhesion to a composite resin. *J Prosthodont Res* 2020; 64:301-6.
- Blatz MB, Sadan A, Kern M. Resin-ceramic bonding: A review of the literature. *J Prosthet Dent* 2003; 89:268-74.
- Borges GA, Sophr AM, de Goes MF, Sobrinho LC, Chan DC. Effect of etching and airborne article abrasion on the microstructure of different dental ceramics. *J Prosthet Dent* 2003; 89:479-88.
- Lopes GC, Perdigão J, Baptista D, Ballarin A. Does a Self-etching Ceramic Primer Improve Bonding to Lithium Disilicate Ceramics? Bond Strengths and FESEM Analyses. *Oper Dent* 2019; 44:210-18.
- Lung CYK, Matinlinna JP. Aspects of silane coupling agents and surface conditioning in dentistry: An overview. *Dent Mater* 2012; 28:467-77.
- Meng Z, Yao X, Yao H, Liang Y, Liu T, Li Y, et al. Measurement of the refractive index of human teeth by optical coherence tomography. *J Biomed Opt* 2009; 14:034010.

- Matsuoka J, Kitamura N, Fujinaga S, Kitaoka T, Yamashita H. Temperature dependence of refractive index of SiO<sub>2</sub> glass. *J Non Cryst Solids* 1991; 135:86-9.
- Matinlinna JP, Lung CYK, Tsoi JKH. Silane adhesion mechanism in dental applications and surface treatments: A review. *Dent Mater* 2018; 34:13-28.
- Debnath S, Wunder SL, McCool JI, Baran GR. Silane treatment effects on glass/resin interfacial shear strengths. *Dent Mat* 2003; 19:441-8.
- Chaijareenont P, Takahashi H, Nishiyama N, Arksornnukit M. Effect of silane coupling agent and solution of different polarity on PMMA bonding to alumina. *Dent Mater J* 2012; 31:610-6.
- Monticelli F, Toledano M, Osorio R, Ferrari M. Effect of temperature on the silane coupling agents when bonding core resin to quartz fiber posts. *Dent Mater* 2006; 22:1024-8.
- Chen B, Lu Z, Meng H, Chen Y, Yang L, Zhang H, et al. Effectiveness of pre-silanization in improving bond performance of universal adhesives or self-adhesive resin cements to silica-based ceramics: Chemical and in vitro evidences. *Dent Mater J* 2019; 35:543-53.
- Babu PJ, Alla RK, Alluri VR, Datla SR, Konakanchi A. Dental Ceramics: Part I C: An Overview of Composition, Structure and Properties. *J Eng Mater Technol* 2015; 3:13-8.
- Shenoy A, Shenoy N. Dental ceramics: An update. *J Conserv Dent* 2010; 13:195-203.
- Matinlinna J, Lassila L, Özcan M, Yli-Urpo A, Vallittu P. An introduction to silanes and their clinical application in dentistry. *Int J Prosthodont* 2004; 17:15-64.
- Nihei T. Dental applications for silane coupling agents. *J Oral Sci*; 58:151-55.
- Nishiyama N, Horie K, Asakura T. Hydrolysis and condensation mechanisms of a silane coupling agent studied by <sup>13</sup>C and <sup>29</sup>Si NMR. *J Appl Polym Sci* 1987; 34:1619-30.
- Savard S, Blanchard LP, Léonard J, Prud'homme RE. Hydrolysis and condensation of silanes in aqueous solutions. *Polymer Composites* 1984; 5:242-9.
- Jiangkongkho P, Arksornnukit M, Takahashi H. The synthesis, modification, and application of nanosilica in polymethyl methacrylate denture base. *Dent Mater J* 2018;37:582-91.

- Salon B, Bayle PA, Abdelmouleh M, Boufi S, Belgacem MN. Kinetics of hydrolysis and self condensation reactions of silanes by NMR spectroscopy. *Colloids and Surfaces A: Physicochemical and Engineering Aspects* 2008; 312:83-91.
- Chen L, Hammond BD, Alex G, Suh BI. Effect of silane contamination on dentin bond strength. *J Prosthet Dent* 2017; 117: 438-43.
- Moro AFV, Ramos AB, Rocha GM, Perez CDR. Effect of prior silane application on the bond strength of a universal adhesive to a lithium disilicate ceramic. *J Prosthet Dent* 2017; 118:666-71.
- Mioche L, Bourdiol P, Monier S. Chewing behavior and bolus formation during mastication of meat with different textures. *Arch Oral Biol* 2003; 48:193-200.
- Nujella BPS, Choudary MT, Reddy SP, Kumar MK, Gopal T. Comparison of shear bond strength of aesthetic restorative materials. *Contemp clin dent* 2012; 3: 22-6.
- Waggoner WF, Cohen H. Failure strength of four veneered primary stainless steel crowns. *Pediatr Dent* 1995; 17: 36-40.
- Rosa WL, Piva E, Silva AF. Bond strength of universal adhesives: A systematic review and meta-analysis. *J Dent* 2015; 43:765-76.
- Gale MS, Darvell BW. Thermal cycling procedures for laboratory testing of dental restorations. *J Dent* 1999; 27:89-99.
- Serichetaphongse P, Chitsutheesiri S, Chengprapakorn W. Comparison of the shear bond strength of composite resins with zirconia and titanium using different resin cements. *J Prosthodont Res* 2021; 65:1-7.
- Alp G, Subaşı MG, Johnston WM, Yilmaz B. Effect of different resin cements and surface treatments on the shear bond strength of ceramic-glass polymer materials. *J Prosthet Dent* 2018; 120:454-61.
- Nasrazadani S, Hassani S. Chapter 2 - Modern analytical techniques in failure analysis of aerospace, chemical, and oil and gas industries. In: Makhoulf ASH, Aliofkhazraei M, editors. *Handbook of Materials Failure Analysis with Case Studies from the Oil and Gas Industry*: Butterworth-Heinemann; 2016. p. 39-54.

- Crouzier L, Delvallee A, Ducourtieux S, Devoille L, Tromas C, Feltin N. A new method for measuring nanoparticle diameter from a set of SEM images using a remarkable point. *Ultramicroscopy*; 2019; 207:112847.
- Harada Y, Ikuhara Y. Chapter 1.1.1 - The Latest Analytical Electron Microscope and its Application to Ceramics. In: Somiya S, editor. *Handbook of Advanced Ceramics*. 2nd ed. Oxford: Academic Press 2013. p. 3-21.
- Arksornnukit M, Takahashi H, Nishiyama N, Effects of silane coupling agent amount on mechanical properties and hydrolytic durability of composite resin after hot water storage. *Dent Mater J* 2004; 23:31-6.
- Nishiyama N, Horie K, Asakura T. Adsorption behavior of a silane coupling agent onto a colloidal silica surface studied by <sup>29</sup>Si NMR spectroscopy. *J Colloid Interface Sci* 1989; 129:113-9.
- Yavuz T, Özyılmaz ÖY, Dilber E, Tobi ES, Kiliç HŞ. Effect of Different Surface Treatments on Porcelain-Resin Bond Strength. *J Prosthodont* 2017; 26:446-54.
- Yoshihara K, Nagaoka N, Sonoda A, Maruo Y, Makita Y, Okihara T, et al. Effectiveness and stability of silane coupling agent incorporated in 'universal' adhesives. *Dent Mater* 2016; 32:1218-1225.
- Kalavacharla VK, Lawson NC, Ramp LC, Burgess JO. Influence of Etching Protocol and Silane Treatment with a Universal Adhesive on Lithium Disilicate Bond Strength. *Oper Dent* 2015; 40:372-378.
- Kim RJY, Woo JS, Lee IB, Yi YA, Hwang JY, Seo DG. Performance of universal adhesives on bonding to leucite-reinforced ceramic. *Biomaterials Research* 2015; 19:1-6.
- Söderholm, K.J., Degradation of Glass Filler in Experimental Composites. *J Dent Res* 1981; 60:1867-75.
- Down Corning Corporation. (2009). *A guide to silane solutions: Silane coupling agents*. United states of America: Down Corning Corporation.
- Shin-Etsu Chemical Co.,Ltd. (2017). *Silane coupling agents: Combination of organic and inorganic materials*. Japan: Shin-Etsu Chemical Co.,Ltd.



**BIOGRAPHY**

มหาวิทยาลัยพระนคร